C H A P T E R

7

GUIDED-WAVE OPTICS

John Tyndall (1820–1893) was the first to demonstrate total internal reflection, which is the basis of guided-wave optics.

Conventional optical instruments make use of light that is transmitted between different locations in the form of beams that are collimated, relayed, focused, or scanned by mirrors, lenses, and prisms. Optical beams diffract and broaden, but they can be refocused by the use of lenses and mirrors. Although such beams are easily obstructed or scattered by various objects, this form of free-space transmission of light is the basis of most optical systems. There is, however, a relatively new technology for transmitting light through dielectric conduits, **guided-wave optics.** It has been developed to provide long-distance light transmission without the use of relay lenses. Guided-wave optics has important applications in directing light to awkward places, in establishing secure communications, and in the fabrication of miniaturized optical and optoelectronic devices requiring the confinement of light.

The basic concept of optical confinement is quite simple. A medium of one refractive index imbedded in a medium of lower refractive index acts as a light "trap" within which optical rays remain confined by multiple total internal reflections at the boundaries. Because this effect facilitates the confinement of light generated inside a medium of high refractive index (see Exercise 1.2-6), it can be exploited in making light conduits—guides that transport light from one location to another. An **optical waveguide** is a light conduit consisting of a slab, strip, or cylinder of dielectric material surrounded by another dielectric material of lower refractive index (Fig. 7.0-1). The light is transported through the inner medium without radiating into the surrounding medium. The most widely used of these waveguides is the optical fiber, which is made of two concentric cylinders of low-loss dielectric material such as glass (see Chap. 8).

Integrated optics is the technology of integrating various optical devices and components for the generation, focusing, splitting, combining, isolation, polarization, coupling, switching, modulation and detection of light, all on a single substrate (chip). Optical waveguides provide the connections between these components. Such chips (Fig. 7.0-2) are optical versions of electronic integrated circuits. Integrated optics has as its goal the miniaturization of optics in much the same way that integrated circuits have miniaturized electronics.
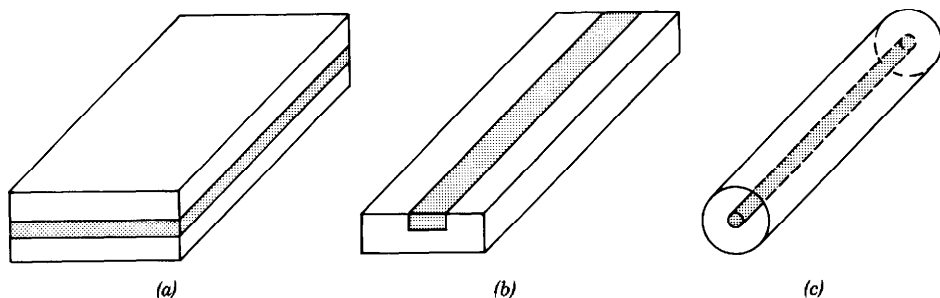

(a)   *(b)*   *(c)*

Figure 7.0-1   Optical waveguides: (*a*) slab; (*b*) strip; (*c*) fiber.
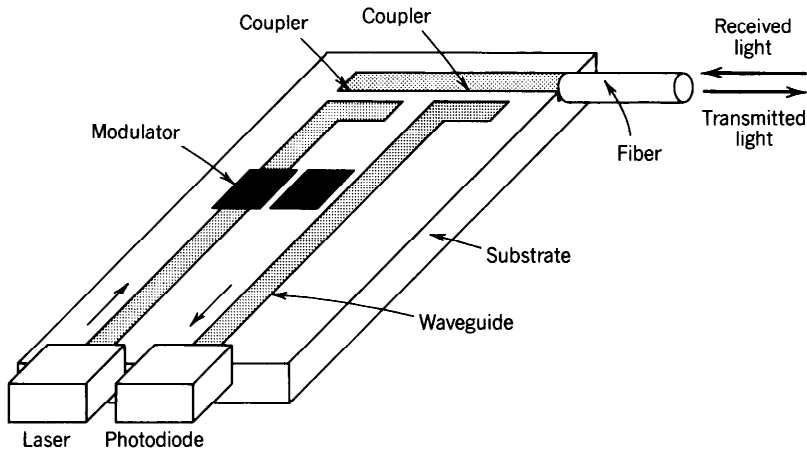
239

Figure 7.0-2 An example of an integrated-optic device used as an optical receiver/transmitter. Received light is coupled into a waveguide and directed to a photodiode where it is detected. Light from a laser is guided, modulated, and coupled into a fiber.

The basic theory of optical waveguides is presented in this and the following chapters. This chapter deals with rectangular waveguides which are used extensively in integrated optics. Cylindrical waveguides, which are used to make optical fibers, are the subject of Chap. 8. Integrated-optic devices (such as semiconductor lasers and detectors, modulators, and switches) are considered in the chapters that deal specifically with those devices. Fiber-optic communication systems are discussed in detail in Chap. 22.

7.1 PLANAR-MIRROR WAVEGUIDES

In this section we examine wave propagation in a waveguide made of two parallel infinite planar *mirrors* separated by a distance *d* (Fig. 7.1-1). The mirrors are assumed ideal; i.e., they reflect light without loss. A ray of light making an angle θ with the mirrors (say in the y–z plane) reflects and bounces between the mirrors without loss of energy. The ray is thus guided along the z direction. This seemingly perfect waveguide is *not* used in practical applications, mainly because of the difficulty and cost of fabricating low-loss mirrors. Nevertheless, this section is devoted to the study of this simple waveguide as a pedagogical introduction to the dielectric waveguide to be
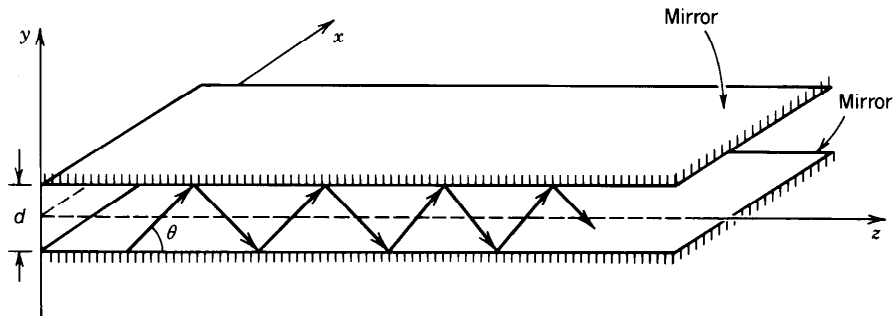

Figure 7.1-1 Planar-mirror waveguide.

examined subsequently in Sec. 7.2 and to the optical resonator, which is the subject of Chap. 9.

Waveguide Modes

The ray-optics picture of light guidance by multiple reflections does not explain a number of important effects that require the use of electromagnetic theory. A simple approach to carrying out an electromagnetic analysis is to associate with each optical ray a transverse electromagnetic (TEM) plane wave. The total electromagnetic field is the sum of these plane waves.

Consider a monochromatic TEM plane wave of wavelength $\lambda = \lambda_o/n$, wavenumber $k = nk_o$, and phase velocity $c = c_o/n$, where n is the refractive index of the medium between the mirrors. The wave is polarized in the x direction and its wavevector lies in the y–z plane at an angle θ with the z axis (Fig. 7.1-1). Like the optical ray, the wave reflects from the upper mirror, travels at an angle $-\theta$, reflects from the lower mirror, and travels once more at an angle θ, and so on. Since the electric field is parallel to the mirror, each reflection is accompanied by a phase shift π, but the amplitude and polarization are not changed. The π phase shift ensures that the sum of each wave and its own reflection vanishes so that the total field is zero at the mirrors. At each point within the waveguide we have TEM waves traveling in the upward direction at an angle θ and others traveling in the downward direction at an angle $-\theta$; all waves are polarized in the x direction.

We now impose a self-consistency condition by requiring that as the wave reflects twice, it reproduces itself [see Fig. 7.1-2(a)], so that we have only two distinct plane waves. Fields that satisfy this condition are called eigenmodes or simply modes of the waveguide (see Appendix C). *Modes are fields that maintain the same transverse distribution and polarization at all distances along the waveguide axis.* We shall see that self-consistency guarantees this shape invariance. In reference to Fig. 7.1-2, the phase shift encountered by the original wave in traveling from A to B must be equal to, or
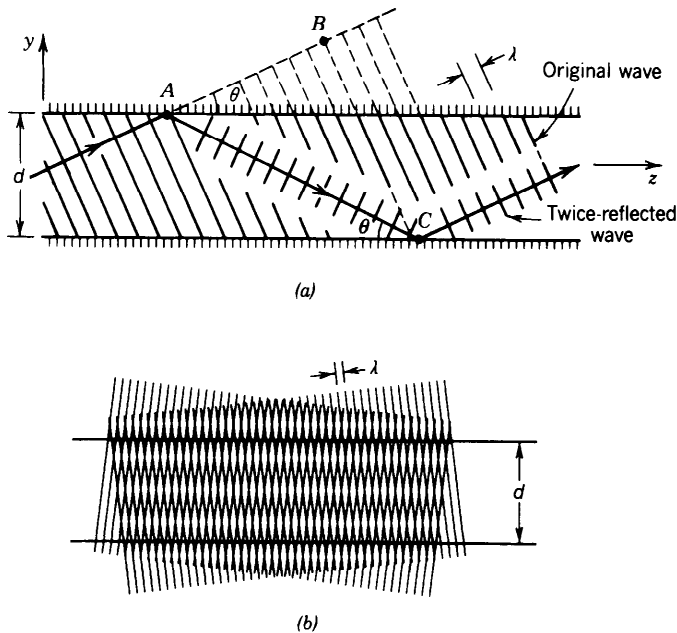

(a)

(b)

Figure 7.1-2 (a) Condition of self-consistency: as a wave reflects twice it duplicates itself. (b) At angles for which self-consistency is satisfied, the two waves interfere and create a pattern that does not change with z.

different by an integer multiple of 2π, from that encountered when the wave reflects, travels from A to C, and reflects once more. Accounting for a phase shift of π at each reflection, we have $2\pi\overline{AC}/\lambda - 2\pi - 2\pi\overline{AB}/\lambda = 2\pi q$, where $q = 0, 1, 2, \ldots$. Since $\overline{AC} - \overline{AB} = 2d \sin\theta$, where d is the distance between the mirrors, $2\pi(2d \sin\theta)/\lambda = 2\pi(q + 1)$, and

$$\frac{2\pi}{\lambda} 2d\sin\theta = 2\pi m, \qquad m = 1, 2, \ldots, \tag{7.1-1}$$

where $m = q + 1$. The self-consistency condition is therefore satisfied only for certain bounce angles $\theta = \theta_m$ satisfying

$$\boxed{\sin\theta_m = m\frac{\lambda}{2d}, \qquad m = 1, 2, \ldots .} \tag{7.1-2}$$
<div align="right">Bounce Angles</div>

Each integer m corresponds to a bounce angle θ_m, and the corresponding field is called the mth mode. The $m = 1$ mode has the smallest angle $\theta_1 = \sin^{-1}(\lambda/2d)$; modes with larger m are composed of more oblique plane-wave components.

When the self-consistency condition is satisfied, the phases of the upward and downward plane waves at points on the z axis differ by half the round-trip phase shift $q\pi$, $q = 0, 1, \ldots$, or $(m - 1)\pi$, $m = 1, 2, \ldots$, so that they add for odd m and subtract for even m.

Since the y component of the propagation constant is $k_y = nk_o \sin\theta$, it is quantized to the values $k_{ym} = nk_o \sin\theta_m = (2\pi/\lambda)\sin\theta_m$. Using (7.1-2), we obtain

$$\boxed{k_{ym} = m\frac{\pi}{d},} \qquad m = 1, 2, 3, \ldots, \tag{7.1-3}$$
<div align="right">Transverse Component
of the Wavevector</div>

so that the k_{ym} are spaced by π/d. Equation (7.1-3) states that the phase shift encountered when a wave travels a distance $2d$ (one round trip) in the y direction, with propagation constant k_{ym}, must be a multiple of 2π.

Propagation Constants

The guided wave is composed of two distinct plane waves traveling at angles $\pm\theta$ with the z axis in the y–z plane. Their wavevectors have components $(0, k_y, k_z)$ and $(0, -k_y, k_z)$. Their sum or difference therefore varies with z as $\exp(-jk_z z)$, so that the propagation constant of the guided wave is $\beta = k_z = k \cos\theta$. Thus β is quantized to the values $\beta_m = k \cos\theta_m$, from which $\beta_m^2 = k^2(1 - \sin^2\theta_m)$. Using (7.1-2), we obtain

$$\boxed{\beta_m^2 = k^2 - \frac{m^2\pi^2}{d^2}.} \tag{7.1-4}$$
<div align="right">Propagation Constants</div>

Higher-order (more oblique) modes travel with smaller propagation constants. The values of θ_m, k_{ym}, and β_m for the different modes are illustrated in Fig. 7.1-3.

Field Distributions

The complex amplitude of the total field in the waveguide is the superposition of the two bouncing TEM plane waves. If $A_m \exp(-jk_{ym}y - j\beta_m z)$ is the upward wave, then $e^{j(m-1)\pi}A_m \exp(+jk_{ym}y - j\beta_m z)$ must be the downward wave [at $y = 0$, the two waves
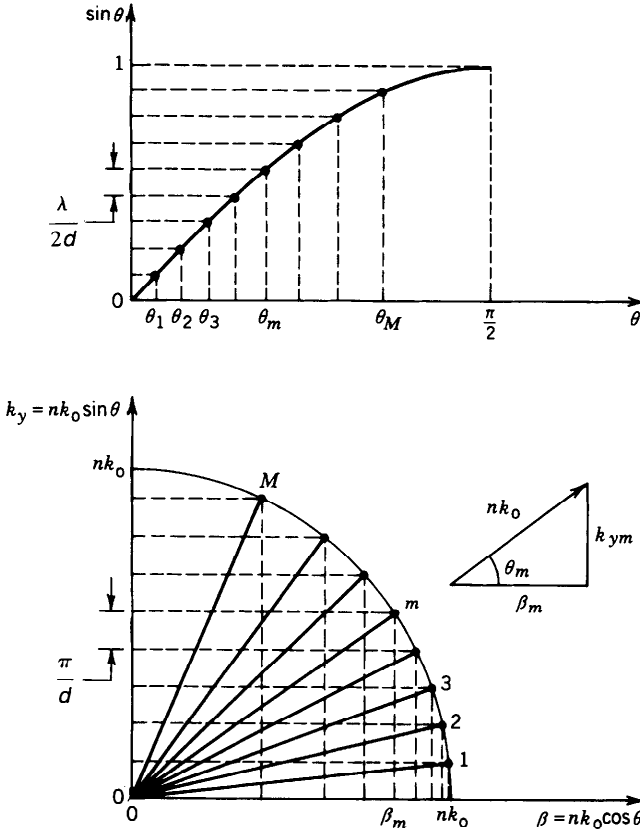
Figure 7.1-3 The bounce angles θ_m and the wavevector components of the modes of a planar-mirror waveguide (indicated by dots). The transverse components $k_{ym} = k \sin \theta_m$ are spaced uniformly at multiples of π/d, but the bounce angles θ_m and the propagation constants β_m are not equally spaced. Mode $m = 1$ has the smallest bounce angle and the largest propagation constant.

differ by a phase shift $(m - 1)\pi$]. There are therefore symmetric modes, for which the two plane-wave components are added, and antisymmetric modes, for which they are subtracted. The total field turns out to be $E_x(y, z) = 2A_m \cos(k_{ym} y) \exp(-j\beta_m z)$ for odd modes and $2jA_m \sin(k_{ym} y) \exp(-j\beta_m z)$ for even modes.

Using (7.1-3) we write the complex amplitude of the electric field in the form

$$E_x(y, z) = a_m u_m(y) \exp(-j\beta_m z), \tag{7.1-5}$$

where

$$u_m(y) = \begin{cases} \sqrt{\dfrac{2}{d}} \cos \dfrac{m\pi y}{d}, & m = 1, 3, 5, \ldots \\[2ex] \sqrt{\dfrac{2}{d}} \sin \dfrac{m\pi y}{d}, & m = 2, 4, 6, \ldots, \end{cases} \tag{7.1-6}$$

and $a_m = \sqrt{2d} \, A_m$ and $j\sqrt{2d} \, A_m$, for odd and even m, respectively. The functions $u_m(y)$ have been normalized to satisfy

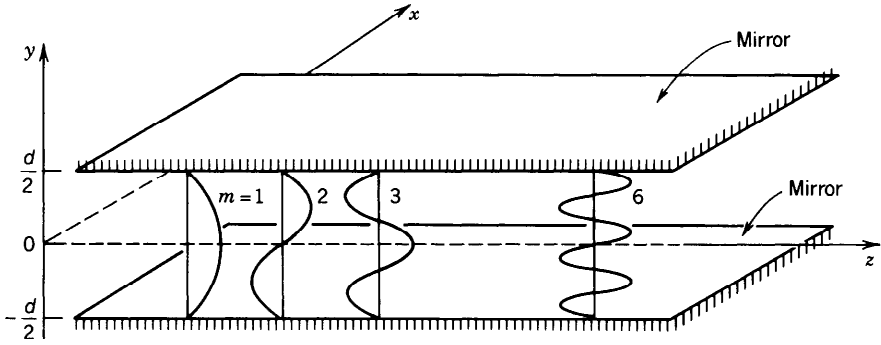$$\int_{-d/2}^{d/2} u_m^2(y) \, dy = 1. \tag{7.1-7}$$

Figure 7.1-4   Field distributions of the modes of a planar-mirror waveguide.

Thus a_m is the amplitude of mode m. It can be shown that the functions $u_m(y)$ also satisfy

$$\int_{-d/2}^{d/2} u_m(y)u_l(y)\, dy = 0, \qquad l \neq m, \tag{7.1-8}$$

i.e., they are orthogonal in the $[-d/2, d/2]$ interval.

The transverse distributions $u_m(y)$ are plotted in Fig. 7.1-4. Each mode can be viewed as a standing wave in the y direction, traveling in the z direction. Modes of large m vary in the transverse plane at a greater rate k_y and travel with a smaller propagation constant β. The field vanishes at $y = \pm d/2$ for all modes, so that the boundary conditions at the surface of the mirrors are always satisfied.

Since we assumed that the bouncing TEM plane wave is polarized in the x direction, the total electric field is also in the x direction and the guided wave is a transverse-electric (TE) wave. Transverse magnetic (TM) waves may be treated similarly, as will be discussed later.

EXERCISE 7.1-1

Optical Power.   Show that the optical power flow in the z direction associated with the TE mode $E_x(y, z) = a_m u_m(y)\exp(-j\beta_m z)$ is $(|a_m|^2/2\eta)\cos\theta_m$ where $\eta = \eta_o/n$ and $\eta_o = (\mu_o/\epsilon_o)^{1/2}$ is the impedance of free space.

Number of Modes

Since $\sin\theta_m = m\lambda/2d$, $m = 1, 2, \ldots$ and for $\sin\theta_m < 1$, the maximum allowed value of m is the greatest integer smaller than $(\lambda/2d)^{-1}$,

$$\boxed{M \doteq \frac{2d}{\lambda}.} \tag{7.1-9}$$

Number of Modes

The symbol $\doteq$ denotes that $2d/\lambda$ is reduced to the nearest integer. For example, when $2d/\lambda = 0.9$, 1, or 1.1, $M = 0$, 0, and 1, respectively. Thus M is the number of
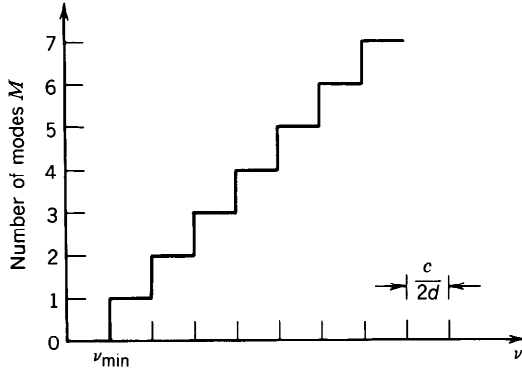
Figure 7.1-5   Number of modes as a function of frequency ν. The cutoff frequency is ν_{min} = $c/2d$. As ν increases by $c/2d$, the number of modes M is incremented by one.

modes of the waveguide. Light can be transmitted through the waveguide in one, two, or many modes. The actual number of modes that carry optical power depends on the source of excitation, but the maximum number is M.

The number of modes increases with increasing ratio of the mirror separation to the wavelength. If $2d/\lambda \leq 1$, $M = 0$, indicating that the self-consistency condition cannot be met and the waveguide cannot support any modes. The wavelength $\lambda_{max} = 2d$ is called the **cutoff wavelength** of the waveguide. It is the longest wavelength that can be guided by the structure. It corresponds to the **cutoff frequency** $\nu_{min} = c/2d$, the lowest frequency of light that can be guided by the waveguide. If $1 < 2d/\lambda \leq 2$ (i.e., $d \leq \lambda < 2d$), only one mode is allowed. The structure is said to be a **single-mode waveguide**. If $d = 5 \mu$m, for example, the waveguide has a cutoff wavelength $\lambda_{max} = 10$ μm; it supports a single mode for 5μm $\leq \lambda < 10 \mu$m, and more modes for $\lambda < 5 \mu$m. Equation (7.1-9) can also be written in terms of the frequency ν, $M \doteq \nu/(c/2d)$, so that the number of modes increases with the frequency ν, as illustrated in Fig. 7.1-5.

Group Velocities

A pulse of light (wavepacket) of angular frequency centered at ω and propagation constant β travels with a velocity $v = d\omega/d\beta$, known as the group velocity (see Sec. 5.6). The propagation constant of mode m is given by (7.1-4) from which $\beta_m^2 = (\omega/c)^2 - m^2\pi^2/d^2$, which is an explicit relation between β_m and ω known as the **dispersion relation**. Taking the derivative and assuming that c is independent of ω (i.e., ignoring dispersion in the waveguide material), we obtain $2\beta_m d\beta_m/d\omega = 2\omega/c^2$, so that $d\omega/d\beta_m = c^2\beta_m/\omega = c^2k \cos\theta_m/\omega = c \cos\theta_m$, from which the group velocity of mode m is

$$v_m = c \cos\theta_m.$$

(7.1-10)
Group Velocity

Thus different modes have different group velocities. More oblique modes travel with a smaller group velocity since they are delayed by the longer path of the zigzaging process.

Equation (7.1-10) may also be obtained geometrically by examining the plane wave as it bounces between the mirrors and determining the distance advanced in the z direction and the time taken by the zigzaging process. For the trip from the bottom
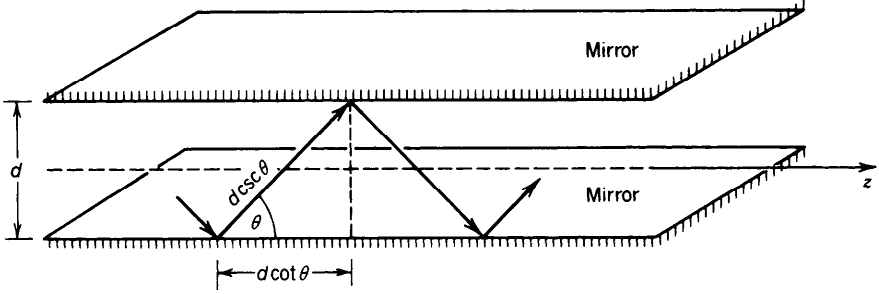
Figure 7.1-6 A plane wave bouncing at an angle θ advances in the z direction a distance $d \cot \theta$ in a time $d \csc \theta / c$. The velocity is $c \cos \theta$.

mirror to the top mirror (Fig. 7.1-6) we have

$$v = \frac{\text{distance}}{\text{time}} = \frac{d \cot \theta}{d \csc \theta / c} = c \cos \theta. \qquad (7.1\text{-}11)$$

TM Modes

The modes considered so far have been TE modes (electric field in the x direction). TM modes (magnetic field in the x direction) can also be supported by the mirror waveguide. They can be studied by means of a TEM plane wave with the magnetic field in the x direction, traveling at an angle θ and reflecting from the two mirrors (Fig. 7.1-7). The electric-field complex amplitude then has components in the y and z directions. Since the z component is parallel to the mirror, it must behave like the x component of the TE mode (i.e., undergo a phase shift π at each reflection and vanish at the mirror). When the self-consistency condition is applied to this component the result is mathematically identical to that of the TE case. The angles θ, the transverse wavevector components k_y, and the propagation constants β of the TM modes associated with this component are identical to those of the TE modes. There are $M = 2d/\lambda$ TM modes (and a total of $2M$ modes) supported by the waveguide.

As previously, the z component of the electric-field complex amplitude of mode m is the sum of an upward plane wave $A_m \exp(-jk_{ym}y)\exp(-j\beta_m z)$ and a downward plane wave $e^{j(m-1)\pi}A_m \exp(jk_{ym}y)\exp(-j\beta_m z)$, with equal amplitudes and phase shift $(m-1)\pi$, so that

$$E_z(y,z) = \begin{cases} a_m \sqrt{\dfrac{2}{d}} \cos \dfrac{m \pi y}{d} \exp(-j\beta_m z), & m = 1,3,5,\ldots \\[2mm] a_m \sqrt{\dfrac{2}{d}} \sin \dfrac{m \pi y}{d} \exp(-j\beta_m z), & m = 2,4,6,\ldots, \end{cases} \qquad (7.1\text{-}12)$$

where $a_m = \sqrt{2d}\, A_m$ and $j\sqrt{2d}\, A_m$ for odd and even m, respectively. Since the electric-field vector of a TEM plane wave is normal to its direction of propagation, it

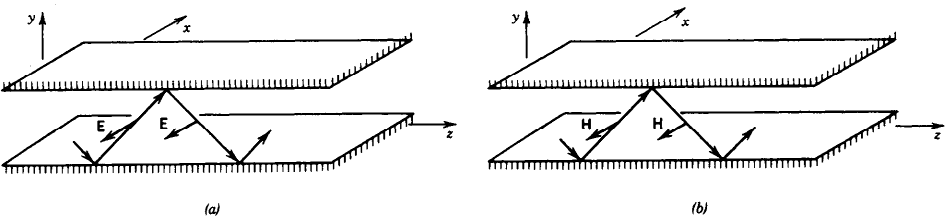(a)   (b)

Figure 7.1-7   Polarization: (a) TE; (b) TM.

makes an angle $\pi/2 + \theta_m$ with the z axis for the upward wave, and $\pi/2 - \theta_m$ for the downward wave.

The y components of the electric field of these waves are

$$A_m \cot \theta_m \exp(-jk_{ym}y)\exp(-j\beta_m z) \quad \text{and} \quad e^{jm\pi}A_m \cot \theta_m \exp(jk_{ym}y)\exp(-j\beta_m z),$$

so that

$$E_y(y,z) = \begin{cases} a_m\sqrt{\dfrac{2}{d}}\,\cot \theta_m \cos\dfrac{m\pi y}{d}\,\exp(-j\beta_m z), & m = 1,3,5,\ldots \\[2mm] a_m\sqrt{\dfrac{2}{d}}\,\cot \theta_m \sin\dfrac{m\pi y}{d}\,\exp(-j\beta_m z), & m = 2,4,6,\ldots. \end{cases} \qquad (7.1\text{-}13)$$

Satisfaction of the boundary conditions is assured because $E_z(y, z)$ vanishes at the mirrors. The magnetic field component $H_x(y, z)$ may be similarly determined by noting that the ratio of the electric to the magnetic fields of a TEM wave is the impedance of the medium η. The resultant fields $E_y(y, z)$, $E_z(y, z)$, and $H_x(y, z)$ do, of course, satisfy Maxwell's equations.

Multimode Fields

It should not be thought that for light to be guided by the mirrors, it must have the distribution of one of the modes. In fact, a field satisfying the boundary conditions
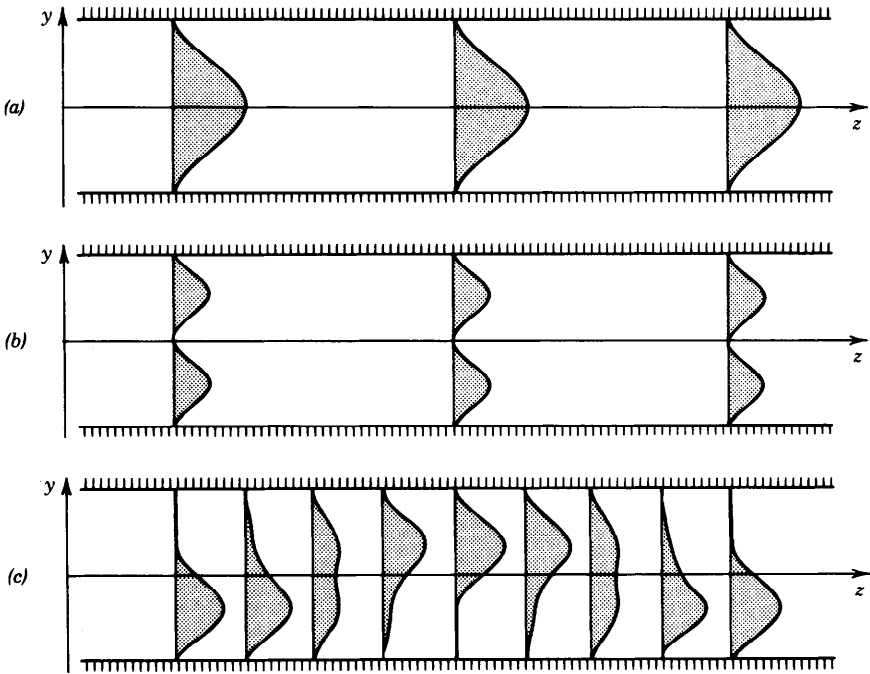

Figure 7.1-8   Variation of the intensity distribution in the transverse direction y at different axial distances z. (a) The electric-field complex amplitude in mode 1 is $E(y, z) = u_1(y)\exp(-j\beta_1 z)$, where $u_1(y) = \sqrt{2/d}\,\cos(\pi y/d)$. The intensity does not vary with z. (b) The complex amplitude in mode 2 is $E(y, z) = u_2(y)\exp(-j\beta_2 z)$, where $u_2(y) = \sqrt{2/d}\,\sin(2\pi y/d)$. The intensity does not vary with z. (c) The complex amplitude in a mixture of modes 1 and 2, $E(y, z) = u_1(y)\exp(-j\beta_1 z) + u_2(y)\exp(-j\beta_2 z)$. Since $\beta_1 \neq \beta_2$, the intensity distribution changes with z.

(vanishing at the mirrors) but otherwise having an arbitrary distribution in the transverse plane *can* be guided by the waveguide. The optical power, however, is divided among the modes. Since different modes travel with different propagation constants and different group velocities, the field changes its transverse distribution as it travels through the waveguide. Figure 7.1-8 illustrates how the transverse intensity distribution of a single mode is invariant to propagation, whereas the multimode distribution varies with z.

An arbitrary field polarized in the x direction and satisfying the boundary conditions can be written as a weighted superposition of the TE modes,

$$E_x(y, z) = \sum_{m=0}^{M} a_m u_m(y) \exp(-j\beta_m z), \qquad (7.1\text{-}14)$$

where a_m, the superposition weights, are the amplitudes of the different modes.

EXERCISE 7.1-2

Optical Power in a Multimode Field. Show that the optical power flow in the z direction associated with the multimode field in (7.1-14) is the sum of the powers $(|a_m|^2/2\eta)\cos\theta_m$ carried by each of the modes.

7.2 PLANAR DIELECTRIC WAVEGUIDES

A planar dielectric waveguide is a slab of dielectric material surrounded by media of lower refractive indices. The light is guided inside the slab by total internal reflection. In thin-film devices the slab is called the "film" and the upper and lower media are called the "cover" and the "substrate," respectively. The inner medium and outer media may also be called the "core" and the "cladding" of the waveguide, respectively. In this section we study the propagation of light in a symmetric planar dielectric waveguide made of a slab of width d and refractive index n_1 surrounded by a cladding of smaller refractive index n_2, as illustrated in Fig. 7.2-1. All materials are assumed to be lossless.

Light rays making angles θ with the z axis, in the y–z plane, undergo multiple total internal reflections at the slab boundaries, provided that θ is smaller than the complement of the critical angle $\bar{\theta}_c = \pi/2 - \sin^{-1}(n_2/n_1) = \cos^{-1}(n_2/n_1)$ [see page 11 and Figs. 6.2-3 and 6.2-5]. They travel in the z direction by bouncing between the slab surfaces without loss of power. Rays making larger angles refract, losing a portion of their power at each reflection, and eventually vanish.

To determine the waveguide modes, a formal approach may be pursued by developing solutions to Maxwell's equations in the inner and outer media with the appropriate boundary conditions imposed (see Problem 7.2-4). We shall instead write the solution in terms of TEM plane waves bouncing between the surfaces of the slab. By imposing the self-consistency condition, we determine the bounce angles of the waveguide modes, from which the propagation constants, field distributions, and group velocities are determined. The analysis is analogous to that used in the previous section for the planar-mirror waveguide.
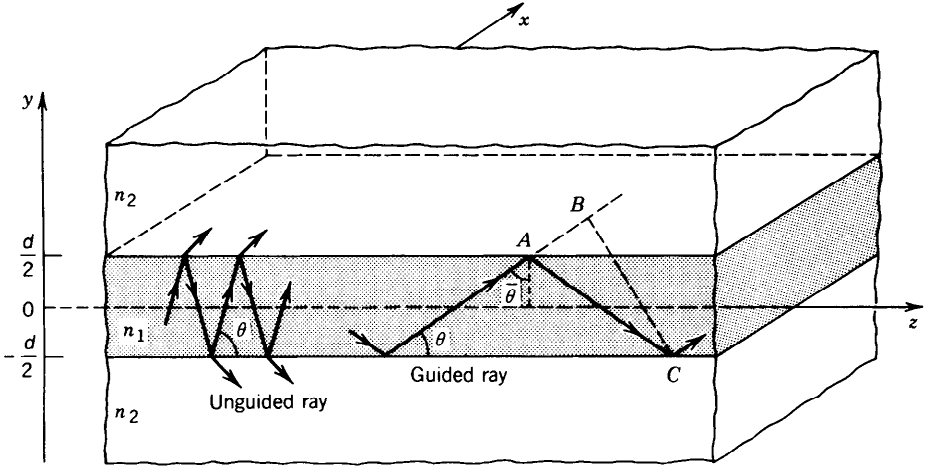
Figure 7.2-1 Planar dielectric waveguide. Rays making an angle $\theta < \bar{\theta}_c = \cos^{-1}(n_2/n_1)$ are guided by total internal reflection.

A. Waveguide Modes

Assume that the field in the slab is in the form of a monochromatic TEM plane wave of wavelength $\lambda = \lambda_o/n_1$ bouncing back and forth at an angle θ smaller than the complementary critical angle $\bar{\theta}_c$. The wave travels with a phase velocity $c_1 = c_o/n_1$, has a wavenumber $n_1 k_o$, and has wavevector components $k_x = 0$, $k_y = n_1 k_o \sin \theta$, and $k_z = n_1 k_o \cos \theta$. To determine the modes we impose the self-consistency condition that a wave reproduces itself after each round trip.

In one round trip, the twice-reflected wave lags behind the original wave by a distance $\overline{AC} - \overline{AB} = 2d \sin \theta$, as in Fig. 7.1-2. There is also a phase φ_r introduced by each internal reflection at the dielectric boundary (see Sec. 6.2). For self-consistency, the phase shift between the two waves must be zero or a multiple of 2π,

$$\frac{2\pi}{\lambda} 2d \sin \theta - 2\varphi_r = 2\pi m, \qquad m = 0, 1, 2, \ldots \tag{7.2-1}$$

or

$$2k_y d - 2\varphi_r = 2\pi m. \tag{7.2-2}$$

The only difference between this condition and the corresponding condition in the mirror waveguide, (7.1-1) and (7.1-3), is that the phase shift π introduced by the mirror is replaced here by the phase shift φ_r introduced at the dielectric boundary.

The reflection phase shift φ_r is a function of the angle θ. It also depends on the polarization of the incident wave, TE or TM. In the TE case (the electric field is in the x direction), substituting $\theta_1 = \pi/2 - \theta$ and $\theta_c = \pi/2 - \bar{\theta}_c$ in (6.2-9) gives

$$\tan \frac{\varphi_r}{2} = \left(\frac{\sin^2 \bar{\theta}_c}{\sin^2 \theta} - 1 \right)^{1/2}, \tag{7.2-3}$$

so that φ_r varies from π to 0 as θ varies from 0 to $\bar{\theta}_c$. Rewriting (7.2-1) in the form
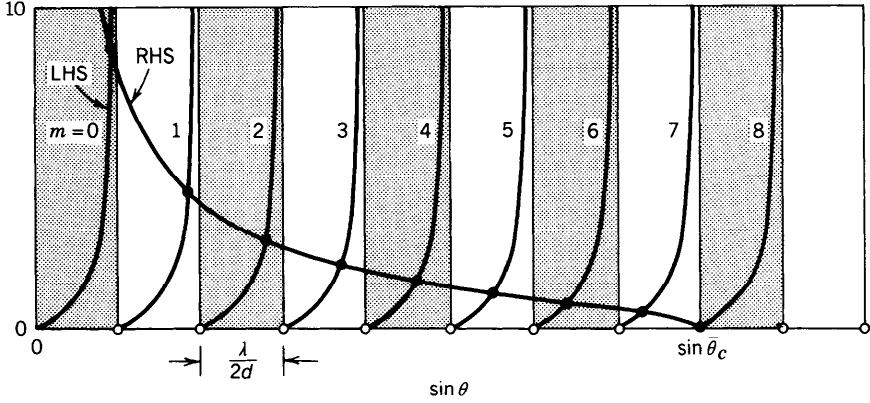
Figure 7.2-2   Graphical solution of (7.2-4) to determine the bounce angles θ_m of the modes of a planar dielectric waveguide. The RHS and LHS of (7.2-4) are plotted versus $\sin\theta$. The intersection points, marked by filled circles, determine $\sin\theta_m$. Each branch of the tan or cot function in the LHS corresponds to a mode. In this plot $\sin\bar{\theta}_c = 8(\lambda/2d)$ and the number of modes is $M = 9$. The open circles mark $\sin\theta_m = m\lambda/2d$, which provide the bounce angles of the modes of a planar-mirror waveguide of the same dimensions.

$\tan(\pi d \sin\theta/\lambda - m\pi/2) = \tan(\varphi_r/2)$ and using (7.2-3), we obtain

$$\tan\left(\pi\frac{d}{\lambda}\sin\theta - m\frac{\pi}{2}\right) = \left(\frac{\sin^2\bar{\theta}_c}{\sin^2\theta} - 1\right)^{1/2}. \qquad (7.2\text{-}4)$$

Self-Consistency
Condition
(TE Modes)

This is a transcendental equation in one variable, $\sin\theta$. Its solutions yield the bounce angles θ_m of the modes. A graphical solution is instructive. The right- and left-hand sides of (7.2-4) are plotted in Fig. 7.2-2 as functions of $\sin\theta$. Solutions are given by the intersection points. The right-hand side (RHS), $\tan(\varphi_r/2)$, is a monotonic decreasing function of $\sin\theta$ which reaches 0 when $\sin\theta = \sin\bar{\theta}_c$. The left-hand side (LHS), generates two families of curves, $\tan[(\pi d/\lambda)\sin\theta]$ and $\cot[(\pi d/\lambda)\sin\theta]$, when m is even and odd, respectively. The intersection points determine the angles θ_m of the modes. The bounce angles of the modes of a *mirror* waveguide of mirror separation d may be obtained from this diagram by using $\varphi_r = \pi$ or, equivalently, $\tan(\varphi_r/2) = \infty$. For comparison, these angles are marked by open circles.

The angles θ_m lie between 0 and $\bar{\theta}_c$. They correspond to wavevectors with components $(0, n_1 k_o \sin\theta_m, n_1 k_o \cos\theta_m)$. The z components are the propagation constants

$$\beta_m = n_1 k_o \cos\theta_m. \qquad (7.2\text{-}5)$$

Propagation Constants

Since $\cos\theta_m$ lies between 1 and $\cos\bar{\theta}_c = n_2/n_1$, β_m lies between $n_2 k_o$ and $n_1 k_o$, as illustrated in Fig. 7.2-3.

The bounce angles θ_m and the propagation constants β_m of TM modes can be found by using the same equation (7.2-1), but with the phase shift φ_r given by (6.2-11). Similar results are obtained.
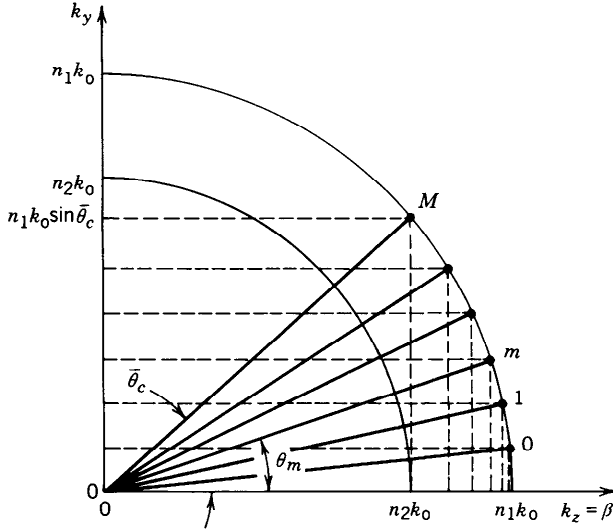
Figure 7.2-3 The bounce angles θ_m and the corresponding components k_z and k_y of the wavevector of the waveguide modes are indicated by dots. The angles θ_m lie between 0 and $\bar{\theta}_c$, and the propagation constants β_m lie between $n_2 k_o$ and $n_1 k_o$. These results should be compared with those shown in Fig. 7.1-3 for the planar-mirror waveguide.

Number of Modes

To determine the number of TE modes supported by the dielectric waveguide we examine the diagram in Fig. 7.2-2. The abscissa is divided into equal intervals of width $\lambda/2d$, each of which contains a mode marked by a filled circle. This extends over angles for which $\sin\theta \leq \sin\bar{\theta}_c$. The number of TE modes is therefore the smallest integer greater than $\sin\bar{\theta}_c/(\lambda/2d)$, so that

$$M \doteq \frac{\sin\bar{\theta}_c}{\lambda/2d}. \tag{7.2-6}$$

The symbol $\doteq$ denotes that $\sin\bar{\theta}_c/(\lambda/2d)$ is increased to the nearest integer. For example, if $\sin\bar{\theta}_c/(\lambda/2d) = 0.9$, 1, or 1.1, $M = 1$, 2, and 2, respectively. Substituting $\cos\bar{\theta}_c = n_2/n_1$ into (7.2-6), we obtain

$$M \doteq 2\frac{d}{\lambda_o}\text{NA}, \tag{7.2-7}$$

Number of TE Modes

where

$$\text{NA} = \left(n_1^2 - n_2^2\right)^{1/2} \tag{7.2-8}$$

Numerical Aperture

is the numerical aperture of the waveguide (the NA is the sine of the angle of acceptance of rays from air into the slab; see Exercise 1.2-5). A similar expression can
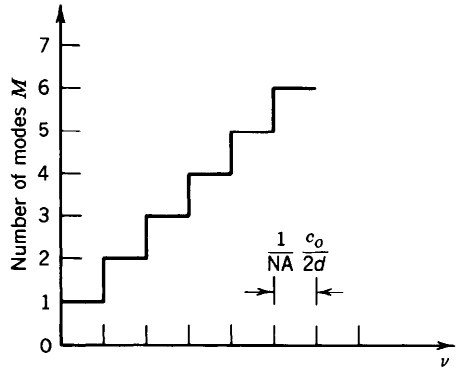
Figure 7.2-4 Number of TE modes as a function of frequency. Compare with Fig. 7.1-5 for the planar-mirror waveguide.

be obtained for the TM modes. If $d/\lambda_o = 10$, $n_1 = 1.47$, and $n_2 = 1.46$, for example, then $\bar{\theta}_c = 6.7°$, NA $= 0.171$, and $M = 4$ TE modes.

When $\lambda/2d > \sin \bar{\theta}_c$ or $(2d/\lambda_o)$NA < 1, only one mode is allowed. The waveguide is then a **single-mode waveguide**. This occurs when the slab is sufficiently thin or the wavelength is sufficiently long. Unlike the mirror waveguide, the dielectric waveguide has no absolute cutoff wavelength (or cutoff frequency). In a dielectric waveguide there is at least one TE mode, since the fundamental mode $m = 0$ is always allowed. Each of the modes $m = 1, 2, \ldots$ has its own cutoff wavelength, however.

The number of modes may also be written as a function of frequency,

$$M \doteq \frac{\mathrm{NA}}{(c_o/2d)} \nu.$$

The relation is illustrated in Fig. 7.2-4. M is incremented by 1 as ν increases by $(c_o/2d)/$NA. Identical expressions for the number of TM modes may be derived similarly.

EXAMPLE 7.2-1.   *Modes in an AlGaAs Waveguide.* A waveguide is made by sandwiching a layer of $\mathrm{Al}_x\mathrm{Ga}_{1-x}\mathrm{As}$ between two layers of $\mathrm{Al}_y\mathrm{Ga}_{1-y}\mathrm{As}$. By changing the concentrations x, y of Al in these compounds their refractive indices are controlled. If x and y are chosen such that at an operating wavelength $\lambda_o = 0.9$ μm, $n_1 = 3.5$, and $n_1 - n_2 = 0.05$, then for a thickness $d = 10$ μm there are $M = 14$ TE modes. For $d < 0.76$ μm, only a single mode is allowed.

B.   Field Distributions

We now determine the field distributions of the TE modes.

Internal Field

The field inside the slab is composed of two TEM plane waves traveling at angles θ_m and $-\theta_m$ with the z axis with wavevector components $(0, \pm n_1 k_o \sin \theta_m, n_1 k_o \cos \theta_m)$. They have the same amplitude and a phase shift $m\pi$ (half that of a round trip) at the center of the slab. The electric-field complex amplitude is therefore $E_x(y, z) = $

$a_m u_m(y) \exp(-j\beta_m z)$, where $\beta_m = n_1 k_o \cos \theta_m$ is the propagation constant, a_m is a constant,

$$
u_m(y) \propto \begin{cases} \cos\left(\dfrac{2\pi \sin \theta_m}{\lambda} y\right), & m = 0, 2, 4, \ldots \\[3mm] \sin\left(\dfrac{2\pi \sin \theta_m}{\lambda} y\right), & m = 1, 3, 5, \ldots, \end{cases} \quad -\frac{d}{2} \leq y \leq \frac{d}{2}, \quad (7.2\text{-}9)
$$

and $\lambda = \lambda_o/n_1$. Note that although the field is harmonic, it does not vanish at the slab boundary. As m increases, $\sin \theta_m$ increases, so that higher-order modes vary more rapidly with y.

External Field

The external field must match the internal field at all boundary points $y = \pm d/2$. It must therefore vary with z as $\exp(-j\beta_m z)$. Substituting $E_x(y, z) = a_m u_m(y) \exp(-j\beta_m z)$ into the Helmholtz equation $(\nabla^2 + n_2^2 k_o^2) E_x(y, z) = 0$, we obtain

$$
\frac{d^2 u_m}{dy^2} - \gamma_m^2 u_m = 0, \tag{7.2-10}
$$

where

$$
\gamma_m^2 = \beta_m^2 - n_2^2 k_o^2. \tag{7.2-11}
$$

Since $\beta_m > n_2 k_o$ for guided modes (see Fig. 7.2-3), $\gamma_m^2 > 0$, so that (7.2-10) is satisfied by the exponential functions $\exp(-\gamma_m y)$ and $\exp(\gamma_m y)$. Since the field must decay away from the slab, we choose $\exp(-\gamma_m y)$ in the upper medium and $\exp(\gamma_m y)$ in the lower medium,

$$
u_m(y) \propto \begin{cases} \exp(-\gamma_m y), & y > \dfrac{d}{2} \\[3mm] \exp(\gamma_m y), & y < -\dfrac{d}{2}. \end{cases} \tag{7.2-12}
$$

The decay rate γ_m is known as the **extinction coefficient**. The wave is said to be an **evanescent wave**. Substituting $\beta_m = n_1 k_o \cos \theta_m$ and $\cos \bar\theta_c = n_2/n_1$, into (7.2-11), we obtain

$$
\boxed{\gamma_m = n_2 k_o \left(\frac{\cos^2 \theta_m}{\cos^2 \bar\theta_c} - 1\right)^{1/2}.} \tag{7.2-13}
$$

Extinction Coefficient

As the mode number m increases, θ_m increases, and γ_m decreases. Higher-order modes therefore penetrate deeper into the cover and substrate.

To determine the proportionality constants in (7.2-9) and (7.2-12), we match the internal and external fields at $y = d/2$ and use the normalization

$$
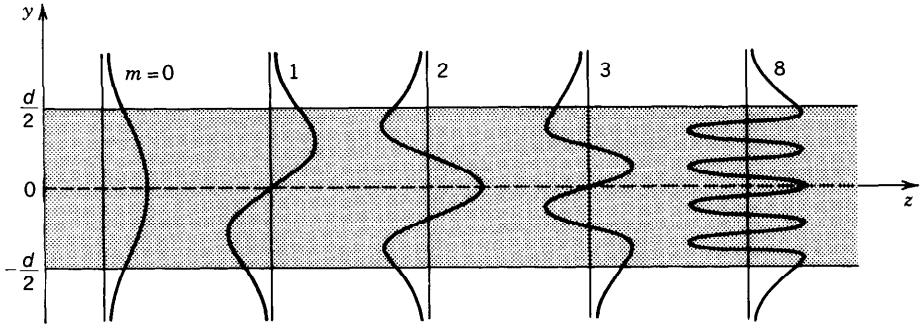\int_{-\infty}^{\infty} u_m^2(y)\, dy = 1. \tag{7.2-14}
$$

Figure 7.2-5 Field distributions for TE guided modes in a dielectric waveguide. These results should be compared with those shown in Fig. 7.1-4 for the planar-mirror waveguide.

This gives an expression for $u_m(y)$ valid for all y. These functions are illustrated in Fig. 7.2-5. As in the mirror waveguide, all of the $u_m(y)$ are orthogonal, i.e.,

$$\int_{-\infty}^{\infty} u_m(y)u_l(y)\, dy = 0, \qquad l \neq m. \tag{7.2-15}$$

An arbitrary TE field in the dielectric waveguide can be written as a superposition of these modes:

$$E_x(y, z) = \sum_m a_m u_m(y) \exp(-j\beta_m z), \tag{7.2-16}$$

where a_m is the amplitude of mode m.

EXERCISE 7.2-1

Confinement Factor. The power confinement factor is the ratio of power in the slab to the total power

$$\Gamma_m = \frac{\int_0^{d/2} u_m^2(y)\, dy}{\int_0^{\infty} u_m^2(y)\, dy}. \tag{7.2-17}$$

Derive an expression for Γ_m as a function of the angle θ_m and the ratio d/λ. Demonstrate that the lowest-order mode (smallest θ_m) has the highest power confinement factor.

The field distributions of the TM modes may be similarly determined (Fig. 7.2-6). Since it is parallel to the slab boundary, the z component of the electric field behaves similarly to the x component of the TE electric field. The analysis may start by determining $E_z(y, z)$. Using the properties of the constituent TEM waves, the other components $E_y(y, z)$ and $H_x(y, z)$ may readily be determined, as was done for mirror waveguides. Alternatively, Maxwell's equations may be used to determine these fields.
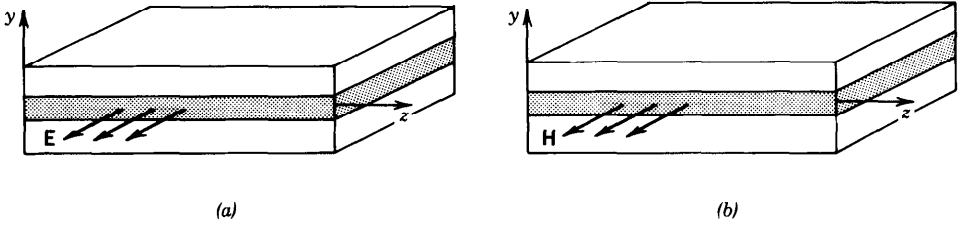
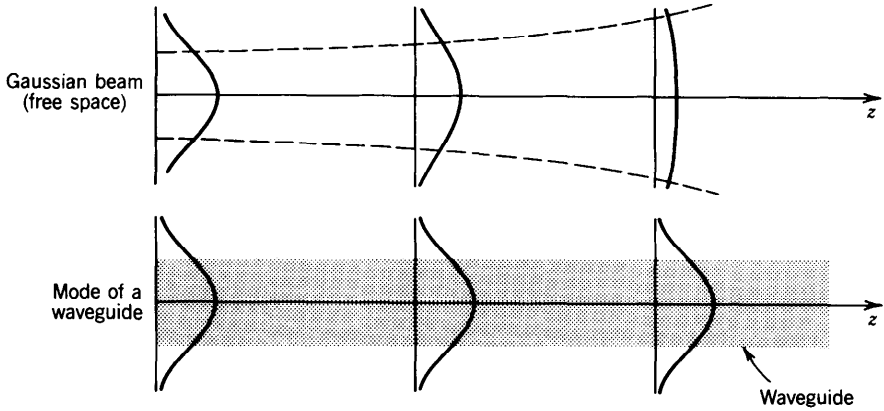**Figure 7.2-6** (a) TE and (b) TM modes in a dielectric planar waveguide.

Figure 7.2-7 Comparison between a Gaussian beam in free space and a waveguide mode.

The field distribution of the lowest-order TE mode ($m = 0$) is similar in shape to that of the Gaussian beam (see Chap. 3). However, unlike the Gaussian beam, guided light does not spread in the transverse direction as it propagates in the axial direction (see Fig. 7.2-7). In a waveguide, the tendency of light to diffract is compensated by the guiding action of the medium.

C. Group Velocities

To determine the group velocity $v = d\omega/d\beta$ for each of the guided modes, we examine the dependence of the propagation constant β on the frequency ω by writing the self-consistency equation (7.2-2) in terms of β and ω. Since $k_y^2 = (\omega/c_1)^2 - \beta^2$, (7.2-2) gives

$$2d\left[\left(\frac{\omega}{c_1}\right)^2 - \beta^2\right]^{1/2} = 2\varphi_r + 2\pi m. \qquad (7.2\text{-}18)$$

Since $\cos \theta = \beta/(\omega/c_1)$ and $\cos \bar{\theta}_c = n_2/n_1 = c_1/c_2$ (7.2-3) becomes

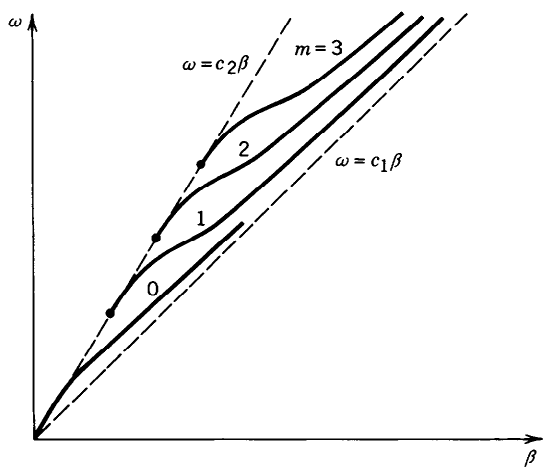$$\tan^2 \frac{\varphi_r}{2} = \frac{\beta^2 - \omega^2/c_2^2}{\omega^2/c_1^2 - \beta^2}. \qquad (7.2\text{-}19)$$

Figure 7.2-8 Schematic of the dispersion relation: angular frequency ω versus propagation constant β, for the different TE modes $m = 0, 1, 2, \ldots$. The group velocity is the slope $v = d\omega/d\beta$. As ω increases the group velocity for each mode decreases from approximately $c_2 = c_o/n_2$ to approximately $c_1 = c_o/n_1$. For $M \gg 1$, at a fixed ω, the group velocities of the different modes extend from approximately c_1 for $m = 0$ to approximately c_2 for $m = M$.

Substituting (7.2-19) into (7.2-18) we obtain

$$\tan^2\left\{\frac{d}{2}\left[\left(\frac{\omega}{c_1}\right)^2 - \beta^2\right]^{1/2} - \frac{m\pi}{2}\right\} = \frac{\beta^2 - \omega^2/c_2^2}{\omega^2/c_1^2 - \beta^2}. \tag{7.2-20}$$

The self-consistency condition therefore establishes a relation between β and ω, the **dispersion relation**. This relation is plotted schematically in Fig. 7.2-8 for the different modes $m = 0, 1, \ldots$.

The group velocities lie between c_1 and c_2 (the phase velocities in the slab and substrate). At a given ω, the lowest-order mode (the least oblique mode, $m = 0$) travels with a group velocity closest to c_1. The most oblique mode $m = M$ has a group velocity $\approx c_2$. This is not surprising. A large portion of the energy carried by the most oblique mode travels in the substrate where the velocity is c_2. Figure 7.2-9 provides a sketch of the group velocities v_m as a function of the mode angle θ_m.
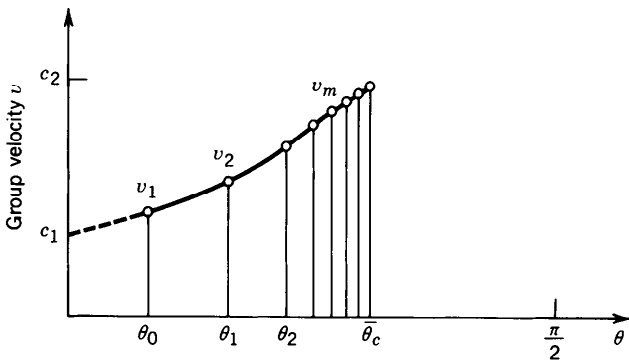

Figure 7.2-9 Group velocities of the waveguide modes. The least oblique mode travels with the smallest group velocity $\approx c_1 = c_o/n_1$. The most oblique mode has a group velocity $\approx c_2 = c_o/n_2$.

EXERCISE 7.2-2

Transit Time.   Show that the maximum disparity between the times taken by the different modes of a planar dielectric waveguide to travel a distance L is

$$\sigma_\tau = \frac{L}{c_1} \Delta, \tag{7.2-21}$$

where $\Delta = (n_1 - n_2)/n_1$. If $n_1 - n_2 = 0.03$, at what distance is the disparity $\sigma_\tau = 1$ ns? Compare this to the case of a mirror waveguide with $n = 1$ and $d/\lambda = 10$. Use (7.1-11), (7.1-2), and (7.1-9).

By taking the total derivative of (7.2-18) with respect to β, we obtain

$$\frac{2d}{2k_y}\left(\frac{2\omega}{c_1^2}\frac{d\omega}{d\beta} - 2\beta\right) = 2\frac{\partial\varphi_r}{\partial\beta} + 2\frac{\partial\varphi_r}{\partial\omega}\frac{d\omega}{d\beta}.$$

Substituting $d\omega/d\beta = v$, $k_y/(\omega/c_1) = \sin\theta$, and $k_y/\beta = \tan\theta$ and introducing the new parameters

$$\Delta z = \frac{\partial\varphi_r}{\partial\beta}, \qquad \Delta\tau = -\frac{\partial\varphi_r}{\partial\omega}, \tag{7.2-22}$$

we obtain

$$v = \frac{d\cot\theta + \Delta z}{d\csc\theta/c_1 + \Delta\tau}. \tag{7.2-23}$$

As we recall from (7.1-11) and Fig. 7.1-6 for the planar-mirror waveguide, $d\cot\theta$ is the distance traveled in the z direction as a ray travels once between the two boundaries. This takes a time $d\csc\theta/c_1$. The ratio $d\cot\theta/(d\csc\theta/c_1) = c_1\cos\theta$ yields the group velocity for the mirror waveguide. The expression (7.2-23) for the group velocity in a dielectric waveguide indicates that the ray travels an additional distance $\Delta z = \partial\varphi_r/\partial\beta$, a trip that lasts a time $\Delta\tau = -\partial\varphi_r/\partial\omega$. We can think of this as an effective penetration of the ray into the cladding, or as an effective lateral shift of the ray, as shown in Fig. 7.2-10. The penetration of a ray undergoing total internal reflection is known as the **Goos–Hänchen effect** (see Problem 6.2-4). Using (7.2-22) it
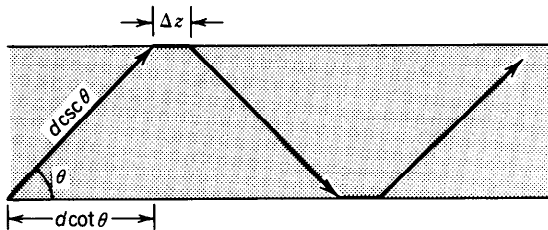

Figure 7.2-10   A ray model that replaces the reflection phase shift with an additional distance Δz traveled at velocity $c_1/\cos\theta$.

can be shown that $\Delta z/\Delta\tau = \omega/\beta = c_1/\cos\theta$. Therefore, more oblique modes travel this lateral distance at a faster speed than less oblique modes. This is responsible for the overall group velocity of more oblique modes being larger (contrary to the case of the mirror waveguide).

EXERCISE 7.2-3

The Asymmetric Planar Waveguide.   Examine the TE field in an asymmetric planar waveguide consisting of a dielectric slab of width d and refractive index n_1 placed on a substrate of lower refractive index n_2 and covered with a medium of refractive index $n_3 < n_2 < n_1$, as illustrated in Fig. 7.2-11.

(a) Determine an expression for the maximum inclination angle θ of plane waves undergoing total internal reflection, and the corresponding numerical aperture NA of the waveguide.
(b) Write an expression for the self-consistency condition, similar to (7.2-4).
(c) Determine an approximate expression for the number of modes M (valid when M is very large).
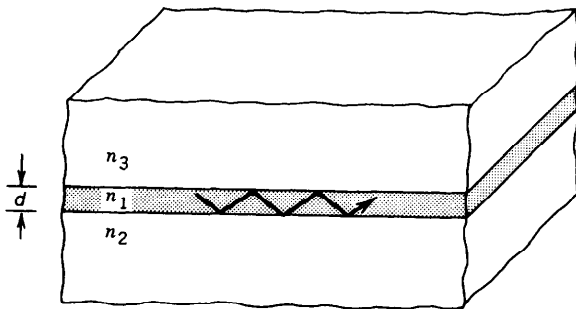

Figure 7.2-11   Asymmetric planar waveguide.

7.3   TWO-DIMENSIONAL WAVEGUIDES

The planar-mirror waveguide and the planar dielectric waveguide studied in the preceding two sections confine light in one transverse direction (the y direction) while guiding it along the z direction. Two-dimensional waveguides confine light in the two transverse directions (the x and y directions). The principle of operation and the underlying modal structure of two-dimensional waveguides is basically the same as planar waveguides; only the mathematical description is lengthier. This section is a brief description of the nature of modes in two-dimensional waveguides. Details can be found in specialized books. Chapter 8 is devoted to an important example of two-dimensional waveguides, the cylindrical dielectric waveguide used in optical fibers.

Rectangular Mirror Waveguide
The simplest generalization of the planar waveguide is the rectangular waveguide (Fig. 7.3-1). If the walls of the guide are mirrors, then, as in the planar case, light is guided
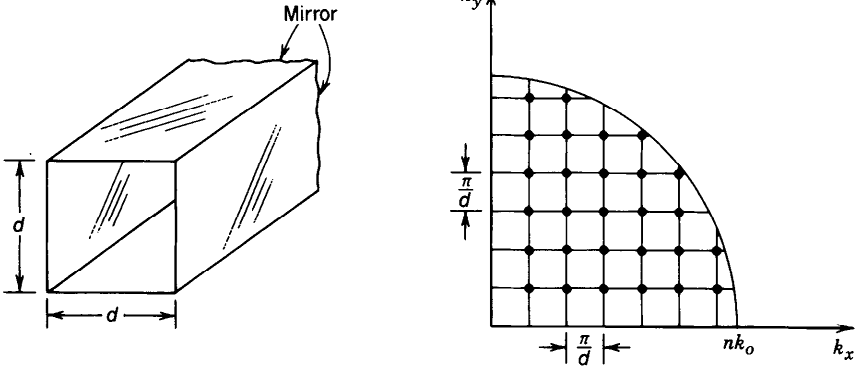
Figure 7.3-1   Modes of a rectangular mirror waveguide are characterized by a finite number of discrete values of k_x and k_y represented by dots.

by multiple reflections at all angles. For simplicity, we assume that the cross section of the guide is a square of width d. If a plane wave of wavevector (k_x, k_y, k_z) and its multiple reflections are to exist self-consistently inside the guide, it must satisfy the conditions:

$$2k_x d = 2\pi m_x, \qquad m_x = 1, 2, \ldots$$

$$2k_y d = 2\pi m_y, \qquad m_y = 1, 2, \ldots, \tag{7.3-1}$$

which are obvious generalizations of (7.1-3).

The propagation constant $\beta = k_z$ can be determined from k_x and k_y by using the relation $k_x^2 + k_y^2 + \beta^2 = n^2 k_o^2$. The three components of the wavevector therefore have discrete values, yielding a finite number of modes. Each mode is identified by two indices m_x and m_y (instead of one index m). All positive integer values of m_x and m_y are allowed as long as $k_x^2 + k_y^2 \leq n^2 k_o^2$, as illustrated in Fig. 7.3-1.

The number of modes M can be easily determined by counting the number of dots within a quarter circle of radius nk_o in the k_x–k_y diagram (Fig. 7.3-1). If this number is large, it may be approximated by the ratio of the area $\pi(nk_o)^2/4$ to the area of a unit cell $(\pi/d)^2$,

$$M \approx \frac{\pi}{4} \left(\frac{2d}{\lambda} \right)^2. \tag{7.3-2}$$

Since there are two polarizations per mode, the total number of modes is actually $2M$. Comparing this to the number of modes in a one-dimensional mirror waveguide, $M \approx 2d/\lambda$, we see that increase of the dimensionality yields approximately the square of the number of modes. The number of modes is a measure of the degrees of freedom. When we add a second dimension we simply multiply the number of degrees of freedom.

The field distributions associated with these modes are generalizations of those in the planar case. Patterns such as those in Fig. 7.1-4 are obtained in each of the x and y directions depending on the mode indices m_x and m_y.

Rectangular Dielectric Waveguide

A dielectric cylinder of refractive index n_1 with square cross section of width d is embedded in a medium of slightly lower refractive index n_2. The waveguide modes can
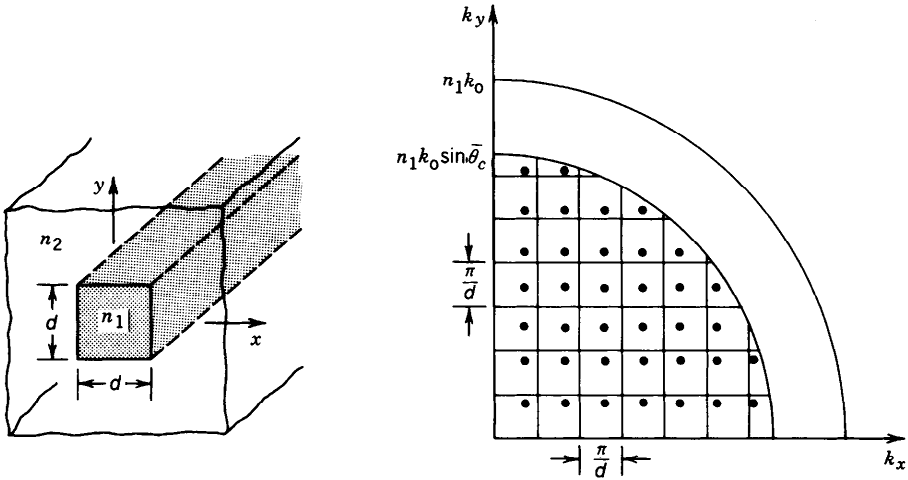
Figure 7.3-2 Geometry of a rectangular dielectric waveguide. The values of k_x and k_y for the waveguide modes are marked by dots.

be determined using a similar theory. Components of the wavevector (k_x, k_y, k_z) must satisfy the condition $k_x^2 + k_y^2 \le n_1^2 k_o^2 \sin^2 \bar{\theta}_c$, where $\bar{\theta}_c = \cos^{-1}(n_2/n_1)$, so that k_x and k_y lie in the area shown in Fig. 7.3-2. The values of k_x and k_y for the different modes can be obtained from a self-consistency condition in which the phase shifts at the dielectric boundary are included, as was done in the planar case.

Unlike the mirror waveguide, k_x and k_y of the modes are not uniformly spaced. However, two consecutive values of k_x (or k_y) are separated by an *average* value of π/d (the same as for the mirror waveguide). The number of modes can therefore be approximated by counting the number of dots in the inner circle in the k_x–k_y diagram of Fig. 7.3-2, assuming an average spacing of π/d. The result is $M \approx (\pi/4)(n_1 k_o \sin \bar{\theta}_c)^2/(\pi/d)^2$, from which

$$M \approx \frac{\pi}{4} \left(\frac{2d}{\lambda_o} \right)^2 \text{NA}^2, \tag{7.3-3}$$

Number of TE Modes

with $\text{NA} = (n_1^2 - n_2^2)^{1/2}$ being the numerical aperture. The approximation is good when M is large. There is also an identical number M of TM modes. Compare this expression with that for the planar dielectric waveguide (7.2-7).

Geometries of Channel Waveguides

Useful geometries for waveguides include the strip, the embedded-strip, the rib or ridge, and the strip-loaded waveguides illustrated in Fig. 7.3-3. The exact analysis for some of these geometries is not easy, and approximations are usually used. The reader is referred to specialized books for further readings on this topic.

The waveguide may be fabricated in different configurations as illustrated in Fig. 7.3-4 for the embedded-strip geometry. S bends are used to offset the propagation axis. The Y branch plays the role of a beamsplitter or combiner. Two Y branches may be used to make a Mach–Zehnder interferometer. Two waveguides in close proximity (or
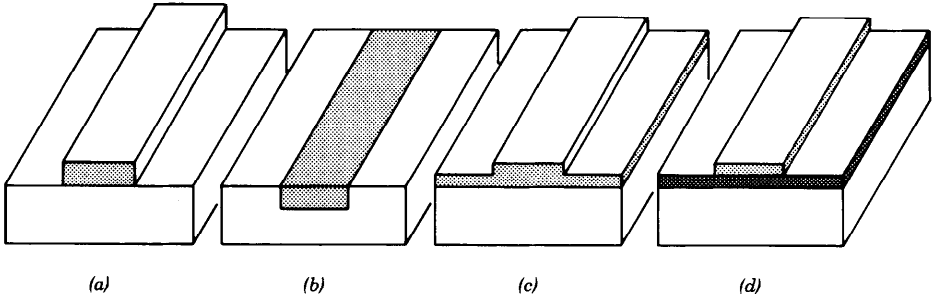
Figure 7.3-3 Various types of waveguide geometries: (a) strip; (b) embedded strip; (c) rib or ridge; (d) strip loaded. The darker the shading, the higher the refractive index.
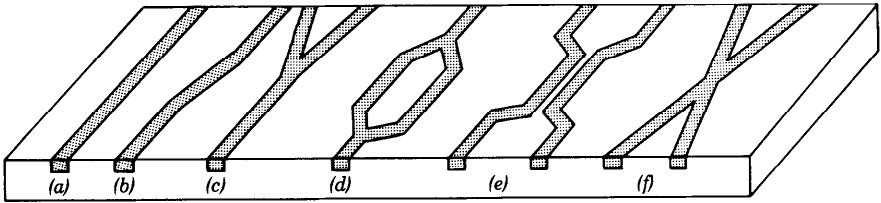

Figure 7.3-4 Different configurations for waveguides: (a) straight; (b) S bend; (c) Y branch; (d) Mach–Zehnder; (e) directional coupler; (f) intersection.

intersecting) can exchange power and may be used as directional couplers, as we shall see in the next section.

The most advanced technology for fabricating waveguides is Ti:LiNbO$_3$. An embedded-strip waveguide is fabricated by diffusing titanium into a lithium niobate substrate to raise its refractive index in the region of the strip. GaAs strip waveguides are made by using layers of GaAs and AlGaAs of lower refractive index. Glass waveguides are made by ion exchange. As we shall see in Chaps. 18 and 21, these waveguides are used to make a number of optical devices, e.g., light modulators and switches.

7.4   OPTICAL COUPLING IN WAVEGUIDES

A.   Input Couplers

Mode Excitation

As was shown in previous sections, light propagates in a waveguide in the form of modes. The complex amplitude of the optical field is generally a superposition of these modes,

$$E(y, z) = \sum_m a_m u_m(y) \exp(-j\beta_m z), \qquad (7.4\text{-}1)$$

where a_m is the amplitude, $u_m(y)$ is the transverse distribution (which is assumed to be real), and β_m is the propagation constant of mode m.

The amplitudes of the different modes depend on the nature of the light source used to "excite" the waveguide. If the source has a distribution that matches perfectly that of a specific mode, only that mode is excited. A source of arbitrary distribution
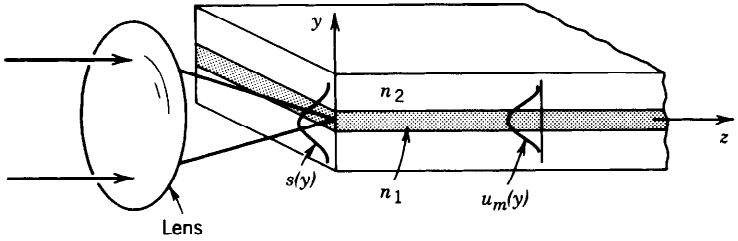
Figure 7.4-1   Coupling an optical beam into a waveguide.

$s(y)$ excites different modes by different amounts. The fraction of power transferred from the source to mode m depends on the degree of similarity between $s(y)$ and $u_m(y)$. We can write $s(y)$ as an expansion (a weighted superposition) of the orthogonal functions $u_m(y)$, i.e.,

$$s(y) = \sum_m a_m u_m(y), \tag{7.4-2}$$

where the coefficient a_l, the amplitude of the excited mode l, is

$$a_l = \int_{-\infty}^{\infty} s(y) u_l(y) \, dy. \tag{7.4-3}$$

This expression can be derived by multiplying both sides of (7.4-2) by $u_l(y)$, integrating with respect to y, and using the orthogonality equation $\int_{-\infty}^{\infty} u_l(y) u_m(y) \, dy = 0$ for $l \neq m$ along with the normalization condition. The coefficient a_l represents the degree of similarity (or correlation) between the source distribution $s(y)$ and the mode distribution $u_l(y)$.

Input Couplers

Light may be coupled into a waveguide by directly focusing it at one end (Fig. 7.4-1). To excite a given mode, the transverse distribution of the incident light $s(y)$ should match that of the mode. The polarization of the incident light must also match that of the desired mode. Because of the small dimensions of the waveguide slab, focusing and alignment are usually difficult and the coupling is inefficient.

In a multimode waveguide, the amount of coupling can be assessed by using a ray-optics approach (Fig. 7.4-2). The guided rays within the waveguide are confined to
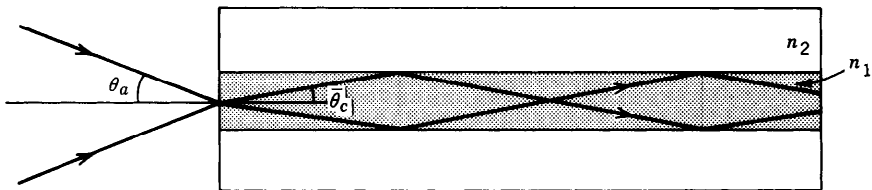

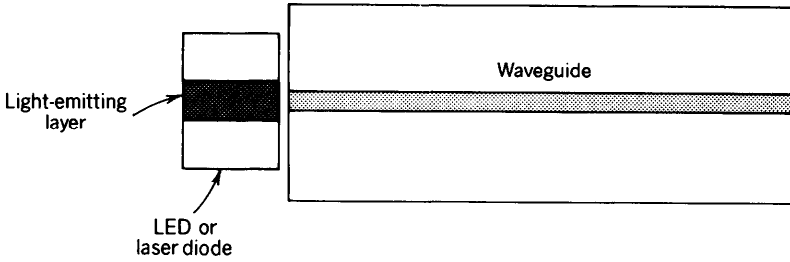**Figure 7.4-2**   Focusing rays into a multimode waveguide.

Figure 7.4-3   End butt coupling a light-emitting diode or a laser diode to a waveguide.

an angle $\bar{\theta}_c = \cos^{-1}(n_2/n_1)$. Because of refraction of the incident rays, this corresponds to an external angle θ_a satisfying NA $= \sin \theta_a = n_1 \sin \bar{\theta}_c = n_1[1 - (n_2/n_1)^2]^{1/2} = (n_1^2 - n_2^2)^{1/2}$, where NA is the numerical aperture of the waveguide (see Exercise 1.2-5). For maximum coupling efficiency the incident light should be focused to an angle not greater than θ_a.

Light may also be coupled from a semiconductor source (a light-emitting diode or a laser diode) into a waveguide simply by aligning the ends of the source and the waveguide while leaving a small space that is selected for maximum coupling (Fig. 7.4-3). In light-emitting diodes, light originates from within a narrow semiconductor junction and is emitted in all directions. In a laser diode, the emitted light is itself confined in a waveguide of its own (light-emitting diodes and laser diodes are described in Chap. 16). Other methods of coupling light into a waveguide include the use of a prism, a diffraction grating, or another waveguide.

The Prism Coupler

Optical power may be coupled into or out of a slab waveguide by use of a prism. A prism of refractive index $n_p > n_2$ is placed at a distance d_p from the slab of a waveguide of refractive indices n_1 and n_2, as illustrated in Fig. 7.4-4. An optical wave is incident into the prism such that it undergoes total internal reflection within the prism at an angle θ_p. The incident and reflected waves form a wave traveling in the z direction with a propagation constant $\beta_p = n_p k_o \cos \theta_p$. The transverse field distribution extends outside the prism and decays exponentially in the space separating the prism and the slab. If the distance d_p is sufficiently small, the wave is coupled to a mode of the slab waveguide with a matching propagation constant $\beta_m \approx \beta_p$. If an appropriate interaction distance is selected, power can be coupled into the slab waveguide, so that the prism acts as an input coupler. The operation may be reversed
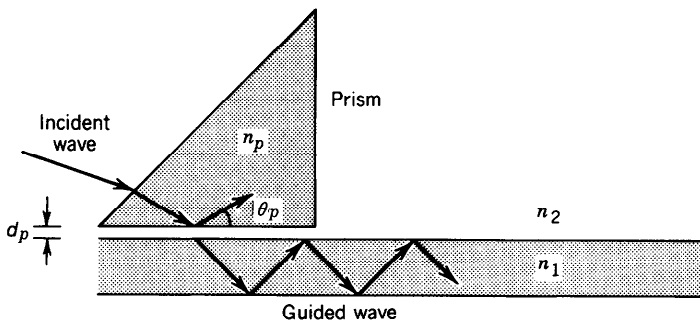

Figure 7.4-4   The prism coupler.

to make an output coupler, which extracts light from the slab waveguide into free space.

B. Coupling Between Waveguides

If two waveguides are sufficiently close such that their fields overlap, light can be coupled from one into the other. Optical power can be transferred between the waveguides, an effect that can be used to make optical couplers and switches. The basic principle of waveguide coupling is presented here; couplers and switches are discussed in Chaps. 21 and 22. Consider two parallel planar waveguides made of two slabs of widths d, separation $2a$, and refractive indices n_1 and n_2 embedded in a medium of refractive index n slightly smaller than n_1 and n_2, as illustrated in Fig. 7.4-5. Each of the waveguides is assumed to be single-mode. The separation between the waveguides is such that the optical field outside the slab of one waveguide (in the absence of the other) overlaps slightly with the slab of the other waveguide.

The formal approach to studying the propagation of light in this structure is to write Maxwell's equations in the different regions and use the boundary conditions to determine the modes of the overall system. These modes are different from those of each of the waveguides in isolation. An exact analysis is difficult and is beyond the scope of this book. However, for weak coupling, a simplified approximate theory, known as coupled-mode theory, is usually satisfactory.

The coupled-mode theory assumes that the modes of each of the waveguides, in the absence of the other, remain approximately the same, say $u_1(y)\exp(-j\beta_1 z)$ and $u_2(y)\exp(-j\beta_2 z)$, and that coupling modifies the *amplitudes* of these modes without affecting their transverse spatial distributions or their propagation constants. The amplitudes of the modes of waveguides 1 and 2 are therefore functions of z, $a_1(z)$ and $a_2(z)$. The theory aims at determining $a_1(z)$ and $a_2(z)$ under appropriate boundary conditions.

Coupling can be regarded as a scattering effect. The field of waveguide 1 is scattered from waveguide 2, creating a source of light that changes the amplitude of the field in waveguide 2. The field of waveguide 2 has a similar effect on waveguide 1. An analysis of this mutual interaction leads to two coupled differential equations that govern the variation of the amplitudes $a_1(z)$ and $a_2(z)$.
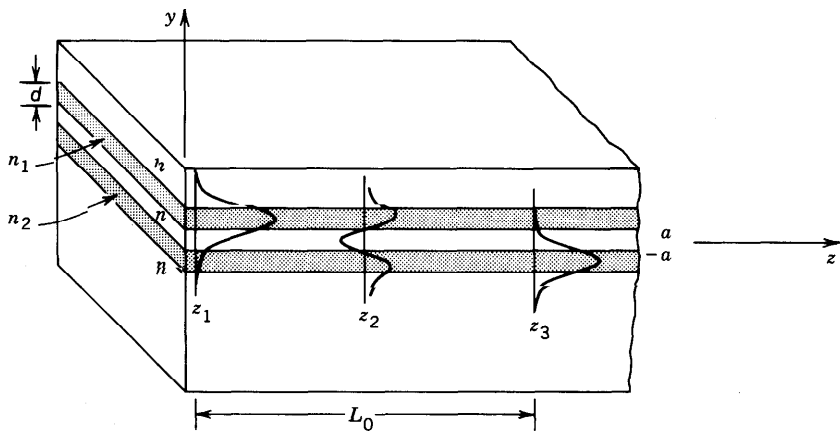

Figure 7.4-5 Coupling between two parallel planar waveguides. At z_1 light is mostly in waveguide 1, at z_2 it is divided equally between the two waveguides, and at z_3 it is mostly in waveguide 2.

It can be shown (see the derivation at the end of this section) that the amplitudes $a_1(z)$ and $a_2(z)$ are governed by two coupled first-order differential equations

$$\frac{da_1}{dz} = -jC_{21} \exp(j\,\Delta\beta\,z)a_2(z) \tag{7.4-4a}$$

$$\frac{da_2}{dz} = -jC_{12} \exp(-j\,\Delta\beta\,z)a_1(z), \tag{7.4-4b}$$

Coupled-Mode
Equations

where

$$\Delta\beta = \beta_1 - \beta_2 \tag{7.4-5}$$

is the phase mismatch per unit length and

$$C_{21} = \frac{1}{2}\left(n_2^2 - n^2\right)\frac{k_o^2}{\beta_1}\int_a^{a+d} u_1(y)u_2(y)\,dy, \tag{7.4-6}$$

$$C_{12} = \frac{1}{2}\left(n_1^2 - n^2\right)\frac{k_o^2}{\beta_2}\int_{-a-d}^{-a} u_2(y)u_1(y)\,dy$$

are coupling coefficients.

We see from (7.4-4) that the rate of variation of a_1 is proportional to a_2, and vice versa. The coefficient of proportionality is the product of the coupling coefficient and the phase mismatch factor $\exp(j\,\Delta\beta\,z)$.

Assuming that the amplitude of light entering waveguide 1 is $a_1(0)$ and that no light enters waveguide 2, $a_2(0) = 0$, then (7.4-4) can be solved under these boundary conditions, yielding the harmonic solution

$$a_1(z) = a_1(0)\exp\left(+\frac{j\,\Delta\beta\,z}{2}\right)\left(\cos\gamma z - j\frac{\Delta\beta}{2\gamma}\sin\gamma z\right) \tag{7.4-7a}$$

$$a_2(z) = a_1(0)\frac{C_{12}}{j\gamma}\exp\left(-j\frac{\Delta\beta\,z}{2}\right)\sin\gamma z, \tag{7.4-7b}$$

where

$$\gamma^2 = \left(\frac{\Delta\beta}{2}\right)^2 + C^2 \tag{7.4-8}$$

and

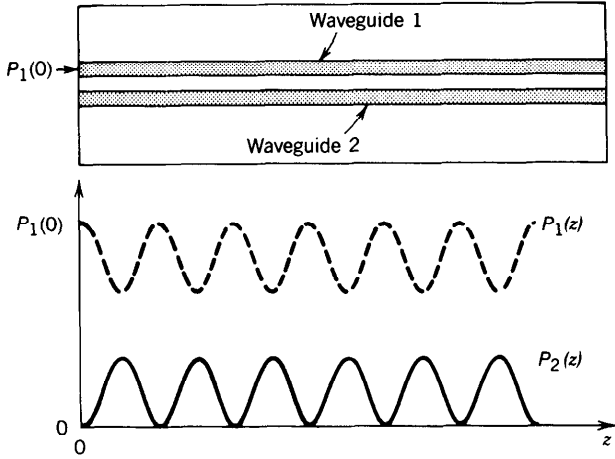$$C = \left(C_{12}C_{21}\right)^{1/2}. \tag{7.4-9}$$

Figure 7.4-6   Periodic exchange of power between guides 1 and 2.

The optical powers $P_1(z) \propto |a_1(z)|^2$ and $P_2(z) \propto |a_2(z)|^2$ are therefore

$$P_1(z) = P_1(0)\left[\cos^2 \gamma z + \left(\frac{\Delta\beta}{2\gamma}\right)^2 \sin^2 \gamma z\right] \qquad (7.4\text{-}10\text{a})$$

$$P_2(z) = P_1(0)\frac{|C_{12}|^2}{\gamma^2} \sin^2 \gamma z. \qquad (7.4\text{-}10\text{b})$$

Thus power is exchanged periodically between the two guides as illustrated in Fig. 7.4-6. The period is $2\pi/\gamma$. Power conservation requires that $C_{12} = C_{21} = C$.

When the guides are identical, i.e., $n_1 = n_2$, $\beta_1 = \beta_2$, and $\Delta\beta = 0$, the two guided waves are said to be phase matched. Equations (7.4-10a, b) then simplify to

$$P_1(z) = P_1(0) \cos^2 Cz \qquad (7.4\text{-}11\text{a})$$

$$P_2(z) = P_1(0) \sin^2 Cz. \qquad (7.4\text{-}11\text{b})$$

The exchange of power between the waveguides can then be complete, as illustrated in Fig. 7.4-7.
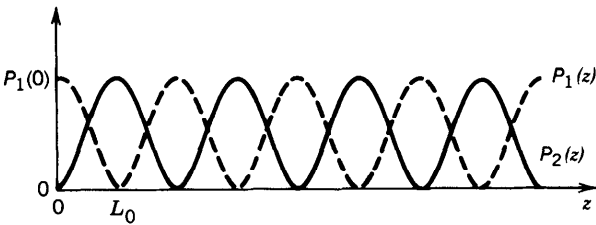

Figure 7.4-7   Exchange of power between guides 1 and 2 in the phase-matched case.
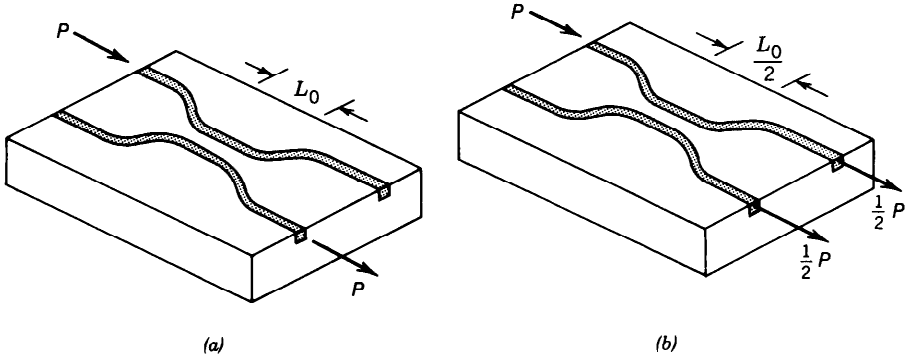
Figure 7.4-8 Optical couplers: (a) switching of power from one waveguide to another; (b) a 3-dB coupler.

We thus have a device for coupling desired fractions of optical power from one waveguide to another. At a distance $z = L_0 = \pi/2\mathcal{C}$, called the transfer distance, the power is transferred completely from waveguide 1 to waveguide 2 [Fig. 7.4-8(a)]. At a distance $L_0/2$, half the power is transferred, so that the device acts as a 3-dB coupler, i.e., a 50/50 beamsplitter [Fig. 7.4-8(b)].

Switching by Control of Phase Mismatch

A waveguide coupler of fixed length, $L_0 = \pi/2\mathcal{C}$, for example, changes its power-transfer ratio if a small phase mismatch $\Delta\beta$ is introduced. Using (7.4-10b) and (7.4-8), the power-transfer ratio $\mathcal{T} = P_2(L_0)/P_1(0)$ may be written as a function of $\Delta\beta$,

$$\mathcal{T} = \left(\frac{\pi}{2}\right)^2 \text{sinc}^2\left\{\frac{1}{2}\left[1 + \left(\frac{\Delta\beta\, L_0}{\pi}\right)^2\right]^{1/2}\right\},$$

(7.4-12)
Power-Transfer
Ratio

where $\text{sinc}(x) = \sin(\pi x)/(\pi x)$. Figure 7.4-9 illustrates the dependence of the power-transfer ratio $\mathcal{T}$ on the mismatch parameter $\Delta\beta\, L_0$. The ratio has a maximum value of unity at $\Delta\beta\, L_0 = 0$, decreases with increasing $\Delta\beta\, L_0$, and then vanishes when $\Delta\beta\, L_0 = \sqrt{3}\,\pi$.
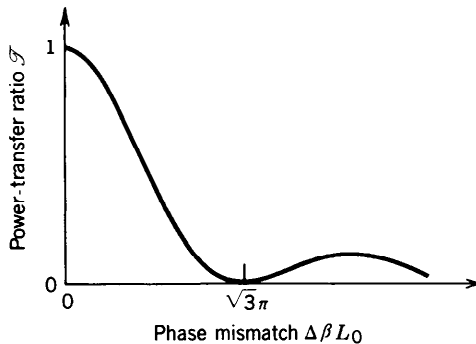

Figure 7.4-9 Dependence of the power transfer ratio $\mathcal{T} = P_2(L_0)/P_1(0)$ on the phase mismatch parameter $\Delta\beta L_0$. The waveguide length is chosen such that for $\Delta\beta = 0$ (the phase-matched case), maximum power is transferred to waveguide 2, i.e., $\mathcal{T} = 1$.

The dependence of the transferred power on the phase mismatch can be utilized in making electrically activated directional couplers. If the mismatch $\Delta\beta L_0$ is switched between 0 and $\sqrt{3}\,\pi$, the light is switched from waveguide 2 to waveguide 1. Electrical control of $\Delta\beta$ can be achieved if the material of the waveguides is electro-optic (i.e., if its refractive index can be altered by applying an electric field). Such a device will be studied in Chaps. 18 and 21 in connection with electro-optic switches.

*Derivation of the Coupled Wave Equations

We now derive the differential equations (7.4-4) that govern the amplitudes $a_1(z)$ and $a_2(z)$ of the coupled modes. When the two waveguides are not interacting they carry optical fields whose complex amplitudes are of the form

$$E_1(y, z) = a_1 u_1(y) \exp(-j\beta_1 z) \tag{7.4-13a}$$

$$E_2(y, z) = a_2 u_2(y) \exp(-j\beta_2 z). \tag{7.4-13b}$$

The amplitudes a_1 and a_2 are then constant. In the presence of coupling, we assume that the amplitudes a_1 and a_2 become functions of z but the transverse functions $u_1(y)$ and $u_2(y)$, and the propagation constants β_1 and β_2, are not altered. The amplitudes a_1 and a_2 are assumed to be slowly varying functions of z in comparison with the distance β^{-1} (the inverse of the propagation constant, β_1 or β_2, which is of the order of magnitude of the wavelength of light).

The presence of waveguide 2 is regarded as a perturbation of the medium outside waveguide 1 in the form of a slab of refractive index $n_2 - n$ and width d at a distance $2a$. The excess refractive index $(n_2 - n)$ and the field E_2 correspond to an excess polarization density $P = (\epsilon_2 - \epsilon)E_2 = \epsilon_o(n_2^2 - n^2)E_2$, which creates a source of optical radiation into waveguide 1 [see (5.2-19)] $\mathscr{S}_1 = -\mu_o\, \partial^2\mathscr{P}/\partial t^2$ with complex amplitude

$$S_1 = \mu_o\omega^2 P = \mu_o\omega^2\epsilon_o\left(n_2^2 - n^2\right)E_2 = \left(n_2^2 - n^2\right)k_o^2 E_2$$

$$= \left(k_2^2 - k^2\right)E_2. \tag{7.4-14}$$

Here ϵ_2 and ϵ are the permittivities associated with the refractive indices n_2 and n, and $k_2 = n_2 k_o$. This source is present only in the slab of waveguide 2.

To determine the effect of such a source on the field in waveguide 1, we write the Helmholtz equation in the presence of a source as

$$\nabla^2 E_1 + k_1^2 E_1 = -S_1 = -\left(k_2^2 - k^2\right)E_2. \tag{7.4-15a}$$

We similarly write the Helmholtz equation for the wave in waveguide 2 with a source generated as a result of the field in waveguide 1,

$$\nabla^2 E_2 + k_2^2 E_2 = -S_2 = -\left(k_1^2 - k^2\right)E_1, \tag{7.4-15b}$$

where $k_1 = n_1 k_o$. Equations (7.4-15a, b) are two coupled partial differential equations which we solve to determine E_1 and E_2. This type of perturbation analysis is valid only for weakly coupled waveguides.

We now write $E_1(y, z) = a_1(z)e_1(y, z)$ and $E_2(y, z) = a_2(z)e_2(y, z)$, where $e_1(y, z) = u_1(y)\exp(-j\beta_1 z)$ and $e_2(y, z) = u_2(y)\exp(-j\beta_2 z)$ and note that e_1 and e_2 must

satisfy the Helmholtz equations,

$$\nabla^2 e_1 + k_1^2 e_1 = 0 \tag{7.4-16a}$$

$$\nabla^2 e_2 + k_2^2 e_2 = 0, \tag{7.4-16b}$$

where $k_1 = n_1 k_o$ and $k_2 = n_2 k_o$ for points inside the slabs of waveguides 1 and 2, respectively, and $k_1 = k_2 = n k_o$ elsewhere. Substituting $E_1 = a_1 e_1$ into (7.4-15a), we obtain

$$\frac{d^2 a_1}{dz^2} e_1 + 2 \frac{da_1}{dz} \frac{de_1}{dz} = -\left(k_2^2 - k^2 \right) a_2 e_2. \tag{7.4-17}$$

Noting that a_1 varies slowly, whereas e_1 varies rapidly with z, we neglect the first term of (7.4-17) compared to the second. The ratio between these terms is $[(d\Psi/dz)e_1]/[2\Psi de_1/dz] = [(d\Psi/dz)e_1]/[2\Psi(-j\beta_1 e_1)] = j(d\Psi/\Psi)/2\beta_1\, dz$ where $\Psi = da_1/dz$. The approximation is valid if $d\Psi/\Psi \ll \beta_1\, dz$, i.e., if the variation in $a_1(z)$ is slow in comparison with the length β_1^{-1}.

We now substitute for $e_1 = u_1 \exp(-j\beta_1 z)$ and $e_2 = u_2 \exp(-j\beta_2 z)$ into (7.4-17), after neglecting its first term, to obtain

$$2\frac{da_1}{dz}(-j\beta_1)u_1(y)e^{-j\beta_1 z} = -\left(k_2^2 - k^2 \right) a_2 u_2(y)e^{-j\beta_2 z}. \tag{7.4-18}$$

Multiplying both sides of (7.4-18) by $u_1(y)$, integrating with respect to y, and using the fact that $u_1^2(y)$ is normalized so that its integral is unity, we obtain

$$\frac{da_1}{dz}e^{-j\beta_1 z} = -j\mathcal{C}_{21}a_2(z)e^{-j\beta_2 z}, \tag{7.4-19}$$

where $\mathcal{C}_{21}$ is given by (7.4-6). A similar equation is obtained by repeating the procedure for waveguide 2. These equations yield the coupled differential equations (7.4-4).

READING LIST

Books

T. Tamir, ed., *Guided-Wave Optoelectronics*, Springer-Verlag, New York, 2nd ed. 1990.

H. Nishihara, M. Haruna, and T. Suhara, *Optical Integrated Circuits*, McGraw-Hill, New York, 1989.

P. Yeh, *Optical Waves in Layered Media*, Wiley, New York, 1988.

L. D. Hutcheson, ed., *Integrated Optical Circuits and Components*, Marcel Dekker, New York, 1987.

D. L. Lee, *Electromagnetic Principles of Integrated Optics*, Wiley, New York, 1986.

S. Solimeno, B. Crosignani, and P. DiPorto, *Guiding, Diffraction, and Confinement of Optical Radiation*, Academic Press, Orlando, FL, 1986.

H. Nolting and R. Ulrich, eds., *Integrated Optics*, Springer-Verlag, New York, 1985.

R. G. Hunsperger, *Integrated Optics: Theory and Technology*, Springer-Verlag, New York, 1982, 2nd ed. 1984.

K. Iga, Y. Kokubun, and M. Oikawa, *Fundamentals of Microoptics*, Academic Press, Tokyo, 1984.

H. Huang, *Coupled Mode Theory as Applied to Microwave and Optical Transmission*, VNU Science Press, Utrecht, The Netherlands, 1984.

S. Martellucci and A. N. Chester, eds., *Integrated Optics: Physics and Applications*, Plenum Press, New York, 1983.

D. Marcuse, *Light Transmission Optics*, Van Nostrand-Reinhold, New York, 2nd ed. 1982.

T. Tamir, ed., *Integrated Optics*, Springer-Verlag, New York, 1979, 2nd ed. 1982.

M. J. Adams, *An Introduction to Optical Waveguides*, Wiley, New York, 1981.

G. H. Owyang, *Foundations of Optical Waveguides*, Elsevier/North-Holland, New York, 1981.

D. B. Ostrowsky, ed., *Fiber and Integrated Optics*, Plenum Press, New York, 1979.

M. S. Sodha and A. K. Ghatak, *Inhomogeneous Optical Waveguides*, Plenum Press, New York, 1977.

M. K. Barnoski, *Introduction to Integrated Optics*, Plenum Press, New York, 1974.

D. Marcuse, *Theory of Dielectric Optical Waveguides*, Academic Press, New York, 1974.

N. S. Kapany and J. J. Burke, *Optical Waveguides*, Academic Press, New York, 1972.

Special Journal Issues

Special issue on integrated optics, *Journal of Lightwave Technology*, vol. 6, no. 6, 1988.

Special section on integrated optics and optoelectronics, *Proceedings of the IEEE*, vol. 75, no. 11, 1987.

Special issue on integrated optics, *IEEE Journal of Quantum Electronics*, vol. QE-22, no. 6, 1986.

Joint special issue on optical guided-wave technology, *IEEE Journal of Quantum Electronics*, vol. QE-18, no. 4, 1982.

Special issue on integrated optics, *IEEE Journal of Quantum Electronics*, vol. QE-13, no. 4, 1977.

Articles

W. J. Tomlinson and S. K. Korotky, Integrated Optics: Basic Concepts and Techniques, in *Optical Fiber Telecommunications II*, S. E. Miller and I. P. Kaminow, eds., Academic Press, New York, 1988.

J. Viljanen, M. Maklin, and M. Leppihalme, Ion-Exchanged Integrated Waveguide Structures, *IEEE Circuits and Devices Magazine*, vol. 1, no. 2, pp. 13–16, 1985.

R. C. Alferness, Guided-Wave Devices for Optical Communication, *IEEE Journal of Quantum Electronics*, vol. QE-17, pp. 946–959, 1981.

R. Olshansky, Propagation in Glass Optical Waveguides, *Reviews of Modern Physics*, vol. 51, pp. 341–368, 1979.

P. K. Tien, Integrated Optics and New Wave Phenomena in Optical Waveguides, *Reviews of Modern Physics*, vol. 49, pp. 361–420, 1977.

H. Kogelnik, An Introduction to Integrated Optics, *IEEE Transactions on Microwave Theory and Techniques*, vol. MTT-23, pp. 2–20, 1975.

PROBLEMS

7.1-1 **Field Distribution.** (a) Show that a single TEM plane wave $E_x(y, z) = A \exp(-jk_y y)\exp(-j\beta z)$ cannot satisfy the boundary conditions, $E_x(\pm d/2, z) = 0$ at all z, in the mirror waveguide illustrated in Fig. 7.1-1.

(b) Show that the sum of two TEM plane waves written as $E_x(y, z) = A_1 \exp(-jk_{y1} y)\exp(-j\beta_1 z) + A_2 \exp(-jk_{y2} y)\exp(-j\beta_2 z)$ does satisfy the boundary conditions if $A_1 = \pm A_2$, $\beta_1 = \beta_2$, and $k_{y1} = -k_{y2} = m\pi/d$, $m = 1, 2, \ldots$.

7.1-2 **Modal Dispersion.** Light of wavelength $\lambda_o = 0.633$ μm is transmitted through a mirror waveguide of mirror separation $d = 10$ μm and $n = 1$. Determine the number of TE and TM modes. Determine the group velocities of the fastest and the slowest mode. If a narrow pulse of light is carried by all modes for a distance of 1 m

in the waveguide, how much does the pulse spread as a result of the differences of the group velocities?

7.2-1   **Parameters of a Dielectric Waveguide.** Light of free-space wavelength $\lambda_o = 0.87\ \mu\text{m}$ is guided by a thin planar film of width $d = 2\ \mu\text{m}$ and refractive index $n_1 = 1.6$ surrounded by a medium of refractive index $n_2 = 1.4$.
(a) Determine the critical angle θ_c and its complement $\bar{\theta}_c$, the numerical aperture NA, and the maximum acceptance angle for light originating in air $(n = 1)$.
(b) Determine the number of TE modes.
(c) Determine the bounce angle θ and the group velocity v of the $m = 0$ TE mode.

7.2-2   **Effect of Cladding.** Repeat Problem 7.2-1 if the thin film is suspended in air $(n_2 = 1)$. Compare the results.

7.2-3   **Field Distribution.** The transverse distribution $u_m(y)$ of the electric-field complex amplitude of a TE mode in a slab waveguide is given by (7.2-9) and (7.2-12). Derive an expression for the ratio of the proportionality constants. Plot the distribution of the $m = 0$ TE mode for a slab waveguide with parameters $n_1 = 1.48$, $n_2 = 1.46$, $d = 0.5\ \mu\text{m}$, and $\lambda_o = 0.85\ \mu\text{m}$, and determine its confinement factor (percentage of power in the slab).

7.2-4   **Derivation of the Field Distributions Using Maxwell's Equations.** Assuming that the electric field in a symmetric dielectric waveguide is harmonic within the slab and exponential outside the slab and has a propagation constant β in both media, we may write $E_x(y, z) = u(y)e^{-j\beta z}$, where

$$u(y) = \begin{cases} A\cos(k_y y + \varphi), & -d/2 \leq y \leq d/2, \\ B\exp(-\gamma y), & y > d/2, \\ B\exp(\gamma y), & y < -d/2. \end{cases}$$

For the Helmholtz equation to be satisfied, $k_y^2 + \beta^2 = n_1^2 k_o^2$ and $-\gamma^2 + \beta^2 = n_2^2 k_o^2$. Use Maxwell's equations to derive expressions for $H_y(y, z)$ and $H_z(y, z)$. Show that the boundary conditions are satisfied if β, γ, and k_y take the values β_m, γ_m, and k_{ym} derived in the text and verify the self-consistency condition (7.2-4).

7.2-5   **Single-Mode Waveguide.** What is the largest thickness d of a planar symmetric dielectric waveguide with refractive indices $n_1 = 1.50$ and $n_2 = 1.46$ for which there is only one TE mode at $\lambda_o = 1.3\ \mu\text{m}$? What is the number of modes if a waveguide with this thickness is used at $\lambda_o = 0.85\ \mu\text{m}$ instead?

7.2-6   **Mode Cutoff.** Show that the cutoff condition for TE mode $m > 0$ in a symmetric slab waveguide with $n_1 \approx n_2$ is approximately $\lambda_o^2 \approx 8n_1\Delta n d^2/m^2$, where $\Delta n = n_1 - n_2$.

7.2-7   **TM Modes.** Derive an expression for the bounce angles of the TM modes similar to (7.2-4). Use a computer to generate a plot similar to Fig. 7.2-2 for TM modes in a waveguide with $\sin\bar{\theta}_c = 0.3$ and $\lambda/2d = 0.1$. What is the number of TM modes?

7.3-1   **Modes of a Rectangular Dielectric Waveguide.** A rectangular dielectric waveguide has a square cross section of area $10^{-2}\ \text{mm}^2$ and numerical aperture NA $= 0.1$. Use (7.3-3) to plot the number of TE modes as a function of frequency ν. Compare your results with Fig. 7.2-4.

7.4-1   **Coupling Coefficient Between Two Slabs.** (a) Use (7.4-6) to determine the coupling coefficient between two *identical* slab waveguides of width $d = 0.5\ \mu\text{m}$, spacing $2a = 1.0\ \mu\text{m}$, refractive indices $n_1 = n_2 = 1.48$, in a medium of refractive index $n = 1.46$, at $\lambda_o = 0.85\ \mu\text{m}$. Assume that both guides are operating in the $m = 0$ TE mode and use the results of Problem 7.2-3 to determine the transverse distributions.
(b) Determine the length of the guides so that the device acts as a 3-dB coupler.